THE BURNING OF SINGLE DROPS OF FUEL IN OXIDIZING ATMOSPHERES

Thesis by

Martin Goldsmith

In Partial Fulfillment of the Requirements

For the Degree of

Doctor of Philosophy

California Institute of Technology

Pasadena, California

1955

ACKNOWLEDGEMENTS

The author takes pleasure in expressing his deepest appreciation to Dr. S. S. Penner, whose advice and suggestions have been invaluable to the progress of this research. Thanks are due also to Dr. H. S. Tsien for critical comments and helpful discussions, and for suggesting the analysis presented in Part III.

Financial support for this research program has been provided by the Daniel and Florence Guggenheim Foundation in the form of Guggenheim Jet Propulsion Fellowships granted to the author for the years 1952-54, and by the Office of Ordnance Research under Contract No. DA-04-495-Ord-446. Grateful acknowledgement is made to both of these organizations.

The author wishes also to thank Miss R. Winkel for the careful preparation of the manuscript.

ABSTRACT

The burning of single, isolated drops of fuel in a quiescent oxidizing atmosphere has been investigated theoretically and experimentally. Two theories are presented. The first, called the diffusion theory, rests on the assumption that the rate of burning is determined by the rate at which the reactants are delivered by diffusion to the flame front surrounding the liquid drop. The second, or thermal theory is based on the assumption that chemical reaction rates govern the rate of burning of the droplet.

The effects on droplet burning rate of changes in the composition, temperature, and pressure of the surrounding oxidizing atmosphere have been investigated experimentally. A preliminary study has also been made of the effect of forced convection on droplet burning.

It is found that the thermal theory of droplet burning does not adequately explain the observed variations in droplet burning rate as the composition and temperature of the surrounding atmosphere are varied. On the other hand, substantial agreement is found between the results of the diffusion theory and experimental data.

TABLE OF CONTENTS

LIST OF FIGURES

NOMENCLATURE

r = radial distance from center of drop

T = temperature

T^* = standard reference temperature (usually 298.16°)

t = time

ρ = density of gas mixture

ρ_ℓ = density of liquid fuel

$(c_p)_K$ = specific heat at constant pressure of gaseous species K

c_ℓ = specific heat of liquid fuel

λ = thermal conductivity

$\Delta\ell$ = specific latent heat of vaporization of fuel

D_K = binary diffusion coefficient for species K

Y_K = weight fraction of species K in gaseous mixture

$\dot{m}_F$ = mass rate of flow of fuel vapor

$(h_K)_T$ = specific enthalpy of species K at temperature T

γ_K = $\dot{m}_K/\dot{m}_F$, ratio of mass rate of flow of species K to the mass rate of flow of fuel vapor

a, b = constants in the expression $(c_p)_F = a + bT$

δ_K = $(c_p)_K/(c_p)_0$, ratio of specific heat of species K to specific heat of oxidizer

$\chi_K = \lambda/D_K(c_p)_K\rho$ = dimensionless parameter

$K' = 2\dot{m}_F/\pi r_\ell \rho_\ell$ = "evaporation constant" defined by Godsave

$q^* - c_\ell (T_\ell - T^*)$ = standard heat of reaction for one gram of liquid fuel and γ_0 grams of gaseous oxidizer, both initially at temperature T^*, forming

		gaseous H_2O and CO_2
$\alpha, \beta, \xi, \Lambda, \psi$	=	computational parameters
E	=	activation energy
R	=	universal gas constant
$\bar{T} = E/R$	=	characteristic temperature
$\eta = dT/dr$	=	temperature gradient
ϕ	=	frequency factor
H	=	heat of reaction
$\mathfrak{R}$	=	weight fraction of fuel vapor in mixture

Subscripts

O	=	oxidizer
F	=	fuel
I	=	inert gas
o	=	condition in ambient gas ($r \rightarrow \infty$)
c	=	condition at combustion zone
ℓ	=	condition at drop surface
i	=	condition at ignition surface
p	=	condition at peak temperature surface

I. INTRODUCTION

The burning of fuel sprays is of importance in such widely different applications as stationary boilers, Diesel engines, gas turbines, and rocket motors. In spite of the diversity of these machines, the combustion problems involved in their design bear marks of similarity. The common factors to be considered include atomization, spray characteristics, evaporation, and mixing, as well as the chemical combustion process itself.

In recent years a great deal of research has been carried out on these individual processes, as well as on the overall fuel spray combustion problem. The increasing use of gas turbines and rockets has been in large part responsible for this research. An excellent review of the current status of knowledge in this field has recently been published by Gerstein[1]*, of the National Advisory Committee for Aeronautics. Gerstein points out that as yet no accurate predictions of spray properties, such as droplet size and velocity distributions, are possible from considerations of spray nozzle configuration, except by empirical correlation. Gerstein further concludes that reliable and complete knowledge is as yet lacking concerning the drag coefficients, evaporation and burning rates, and their interrelations, for the droplets in a fuel spray.

However, some progress has been made on these problems for the case of an isolated droplet. Research on isolated, single drops has been motivated by the hope that a more complete understanding of this

---

* Numbers in parentheses refer to references on page 75.

simpler problem will lead to correspondingly greater understanding of the vastly more complex problems of spray burning and combustion chamber design. Also, the results of single drop studies may suggest fruitful avenues of research on the larger scale problems.

Typical of the research done on the problem of evaporation from droplets is the work of Ranz and Marshall[2], who have published extensive data relating to the evaporation rate of a droplet in a gas stream. Ingebo[3, 4] has also made measurements of this nature and has further considered the problem of evaporation rates and drag coefficients for sprays of droplets[5].

The pioneering work on the burning of single fuel drops surrounded by an oxidizing atmosphere was done by Spalding[6] and Godsave[7] in Great Britain. Many of the concepts concerning the physical processes occurring in droplet combustion were first enunciated by Spalding[6], who performed experiments on the burning of liquid films covering solid surfaces. Spalding obtained a semi-quantitative interpretation of his results, using the concept of stagnant gaseous films separating the liquid surface from the surrounding air. He postulated that the flame sheet was separated from the liquid by a stagnant film through which the heat necessary to evaporate the liquid fuel was conducted. In this formulation it was also assumed that the flame was separated from the surrounding air by another stagnant film through which the oxygen necessary for combustion was transported to the flame by diffusion. In this theory, the rate of consumption of the liquid fuel is controlled by the rates of transport of the reactants to the

flame zone, rather than by the chemical reaction rate itself.

The formalization of these ideas was greatly advanced by Godsave[7]. To study the burning of a single fuel droplet experimentally, Godsave suspended such a drop from the slightly thickened lower tip of a fine quartz filament. After the drop was ignited by means of a small gas flame, motion pictures were taken of the drop as it burned and grew smaller. From measurements made of the size of the drop image recorded on the film, Godsave was able to calculate the mass burning rate of the fuel droplet. At the same time, photographs were made of the flame front surrounding the droplet. After making such measurements for various pure hydrocarbon fuels burning in still air, Godsave arrived at the following important conclusions. First, he observed quantitatively that the mass rate of burning of a drop of a given fuel was proportional to the droplet diameter. Secondly, he observed that the flame front surrounding the droplet, as shown in Figure 1, appeared thin, and was separated from the drop surface by a considerable distance, on the order of a drop diameter. This last observation led Godsave to postulate that burning takes place in the form of a diffusion flame surrounding the liquid droplet.

The concept of the so-called diffusion flame was first discussed by Burke and Schuman[8] in 1928. The fundamental concept of the diffusion flame is that combustion takes place in a thin zone that lies between the separate fuel and oxidizer. In this theory, it is assumed that the rate of burning is not governed by chemical kinetics considerations, but rather by the rate at which the reactants are transported to

the combustion zone. The diffusion flame is therefore a transport-controlled flame. These assumptions require, for instance, that no fuel or oxidizer should cross the flame front, but should be always separated by the flame. The spectroscopic measurements of Wolfhard and Parker[9], concerning the structure of diffusion flames, and the gas sampling technique employed by Hottel and Hawthorne[10] in studies of diffusion flames substantiate this fact, hence lend great weight to the fundamental assumptions used in the analysis.

Godsave's observations led him to conclude that fuel vapor was evaporated from the drop and that the vapor flowed outward towards the flame zone, while the oxygen in the surrounding air diffused inward. The rate of burning was then simply the evaporation rate of the liquid fuel and this would, in turn, be determined by the rate of heat transfer to the drop surface from the surrounding hot flame front.

To try to check the validity of his ideas, Godsave constructed an idealized theoretical model of a burning drop. It was assumed that a spherical flame zone surrounded the spherical drop. This flame front was taken to be infinitely thin, or a geometrical surface, and acted as a source of heat to evaporate liquid from droplet. The mathematical calculation for steady-state conditions involved the integration of the conventional second order differential equation for heat transfer, or temperature distribution, which in this case included, in addition to the Laplacian operator, a convection term arising from the outward flow of fuel vapor. As a boundary condition, the heat transferred to the drop was equated to that necessary to supply the latent heat of vaporization.

Godsave solved the resulting equations for the mass burning rate, obtaining this quantity in terms of the drop diameter and the unknown parameters of flame temperature and diameter. The surface temperature of the droplet, which might be assumed to be the boiling temperature, also appears. The various physical properties of the system, such as specific heat and thermal conductivity, were assumed constant for the purposes of the analysis. The final form of Godsave's equation for mass burning rate is

$$\dot{m}_F = \frac{4\pi\lambda r_\ell}{(c_p)_F} \quad \frac{\ln\left\{1 + \left[(c_p)_F (T_c - T_\ell)/\Delta\ell\right]\right\}}{\left[1 - (r_\ell / r_c)\right]} , \qquad (1)$$

where $\dot{m}_F$ is the mass burning rate of the droplet of radius r_ℓ and temperature (near boiling) T_ℓ ; λ is the mean thermal conductivity of the mixture surrounding the drop; $(c_p)_F$ is the mean specific heat of the fuel vapor; $\Delta\ell$ is the specific latent heat of vaporization of the liquid fuel; r_c and T_c are the radius and temperature, respectively, of the flame zone.

From his examination of the motion pictures taken of the burning drops, Godsave concluded that the ratio of flame size to drop size should be taken as a constant. Estimating this quantity from the photographs by constructing a circle to best fit the much elongated flame (elongated due to the effects of free convection), and assuming a reasonable value for the flame temperature (several hundred degrees below the adiabatic flame temperature), Godsave calculated burning rates that were in close agreement with the experimental data. It is seen from Equation (1)

above that with the assumptions of constant ratio of flame to drop size and constant flame temperature, the functional dependence of burning rate on droplet diameter corresponds to that determined by the experiments.

Godsave did not carry on any further with experimental or theoretical work on this problem. It should be noted that several reports have been published in Japan[11, 12] that contain experimental data similar to that of Godsave. A number of other papers pertaining to droplet combustion are also listed in the references (13-17).

It should be noted that an alternate experimental method has been used to study the burning rates of fuel droplets. For instance, in the investigations of Lorell and Wise[18], a porous alundum sphere mounted on fine steel tubing was fed with liquid fuel. A liquid film was thereby maintained over the surface of the sphere, which could then be ignited and would burn in the same fashion as a liquid droplet. The flow of fuel to the sphere was adjusted so that the liquid film was maintained over the surface. The mass burning rate is then equal to the rate of fuel flow to the porous sphere. The results of these experiments, made with spheres of various diameters, again indicate that the mass burning rate is proportional to droplet diameter. The numerical values of the constant of proportionality found by this method are in substantial agreement with the values found from the experiments made on suspended liquid drops.

The purpose of the present investigation is to continue the analytical study of the problem of droplet combustion and to provide

further experimental measurements of droplet burning rates for various pure fuels as some of the environmental conditions, such as pressure, temperature, and composition of the surrounding oxidizing gas are changed. In the following section, a theory for the burning of a droplet in a still atmosphere is presented. While the physical concepts remain the same, this method of analysis differs from that of Godsave in that only integrated forms for the energy and continuity equations are used. This simplifies the analytical treatment, since only first order differential equations occur. Because of the improvement in the method of formulating the problem, it is possible to derive without difficulty an explicit expression for the mass rate of fuel consumption without introducing the invalid approximations that the thermal conductivity and the specific heat of the fuel vapor are independent of the temperature. Furthermore, Godsave's analysis is extended in two important respects by obtaining explicit expressions for the temperature of the combustion surface and the radius of the combustion surface.

In the subsequent section, an alternative theory is presented. In contrast to the above-mentioned theory, where transport phenomena govern the drop burning rate, this second theory, first proposed by Y. H. Kuo[19], is based on the assumption that chemical reaction rates are the controlling factors. The assumptions and analysis strongly resemble the so-called thermal theory for laminar flame propagation[20]. Therefore, for convenience, this latter theory will be referred to as the thermal theory, while the first theory will be referred to as the diffusion theory.

In Section IV, experimental studies of droplet burning are reported. The burning rates of droplets of various common hydrocarbon fuels were measured as the temperature and pressure of the surrounding air were increased. Also, the influence of change in oxygen concentration in the atmosphere was investigated. Preliminary investigation was made of the influence of gas motion (forced convection) past the burning drop. In the concluding section, the results of the experiments are compared with the predictions of the two theories. The experimental evidence is preponderantly in favor of the diffusion theory.

II. DIFFUSION THEORY FOR DROPLET BURNING[21]

Following Spalding[6] and Godsave[7], the following mechanism is postulated for the combustion process: oxidizer is delivered from the surrounding atmosphere to the region of active combustion by convection and diffusion; the fuel evaporates and diffuses, without chemical change, to the reaction front, which is assumed to be a spherical shell surrounding the droplet. The location of the reaction front is defined by the condition that the ratio of the mass rate of delivery of fuel to oxidizer corresponds to stoichiometric proportions. It is assumed that the reactants are consumed instantaneously upon reaching the flame front. The problem of determining the rate of burning therefore reduces to that of finding the solutions of the appropriate transfer problems. Because it is to be expected that the rates of mass and heat transfer will be increased by the effects of convection, a lower limit for the burning rate will be obtained if the analysis is made for a droplet burning in a still atmosphere, by neglecting the convection of hot gases over the fuel droplet. Although fuel may be injected into the combustion chamber of an engine at a velocity appreciably different from the gas velocity in the chamber, it is apparent that the droplet must be rapidly slowed down to the local gas velocity because of aerodynamic drag. This effect becomes more pronounced for smaller droplets, as the mass of a drop is proportional to the cube of the diameter, and the aerodynamic force is roughly proportional to the diameter, for laminar flow over the small sphere. Hence, for decreasing sizes of drops, the rates of acceleration must increase.

For the sake of clarity, all important assumptions upon which the present diffusion theory analysis is based are tabulated below. These are:

1. The droplets are spherical.
2. Convection effects will be neglected.
3. As a corollary of the preceding assumption, spherical symmetry prevails and the flame front surrounding the drop is represented by a spherical surface concentric with the drop. All reactions take place instantaneously at this surface, and its location is defined by the requirement that the rates of delivery of fuel and oxidizer are in the stoichiometric ratio.
4. Steady-state conditions are assumed for fixed droplet sizes. This restriction greatly facilitates the mathematical treatment. Physically, the assumption will be valid if the burning time of the droplet is very much longer than the characteristic time τ for the transport processes. Here τ can be estimated to be d^2/k, where d is the droplet diameter and k is the thermal diffusivity. For the typical values of $d = 0.1$ cm and $k = 1$ cm^2/sec, $\tau = 10^{-2}$ seconds, which is small in comparison to the typical burning time of 1 second for a droplet of this size. It is reasonable then to assume that the solution obtained for a fixed size applies to a drop decreasing in size when it reaches the radius used in the steady-state solution.

5. The effect of heat transfer by radiation is neglected.
6. Mean values will be used, when appropriate, for the physical properties.
7. The temperature of the liquid drop is assumed to be uniform and equal to the boiling temperature. Although this assumption is questionable[14], it does not exert a large effect on the theoretical results, as will be shown in the subsequent analysis.
8. The pressure is assumed to be uniform throughout the system, due to the smallness of the inertia forces. The validity of this assumption is shown in detail in Appendix A.

A schematic diagram of an evaporating and burning fuel droplet in an oxidizing atmosphere is shown in Figure 2. The radius of the liquid drop is r_ℓ and its temperature is the normal boiling point T_ℓ. The radial distance of the combustion surface from the center of the liquid droplet is r_c and its temperature is T_c. The oxygen-inert gas mixture at a large distance from the combustion surface is at the temperature T_o. In order to clarify further the physical picture, temperature and concentration profiles have been computed according to the diffusion theory. A plot of the temperature (T) as a function of the radial distance (r) from the center of the drop is shown in Figure 3a. In Figures 3b to 3d, diagrams of the weight fractions of fuel (Y_F), oxidizer (Y_O), and inert gas (Y_I) are shown as a function of (r). The data shown in Figures 3a to 3d correspond to the burning of a droplet of benzene in air for $r_\ell = 0.005$ cm and $T_o = 300^oK$. The

profile for the weight fraction of inert gas has been drawn on the assumption that the physical properties of combustion products and inert gas (in the oxidizer-inert gas mixture) are alike. If this assumption is not made, we must treat ternary gas mixtures both for $r \gtrless r_c$ and for $r \lessgtr r_c$. This refinement can be introduced without difficulty, but does not appear to be warranted in view of other approximations in the analysis.

Let $\dot{m}_F$ represent the steady-state mass rate of fuel consumption, which is the desired eigenvalue of our boundary-value problem; t is the time; ρ, c_p, and λ represent, respectively, the density, specific heat at constant pressure, and thermal conductivity; $\Delta\ell$ equals the specific latent heat of evaporation of the fuel.

For a constant-pressure flow process,* the first law of thermodynamics leads to the relation

$$\rho\,(Dh/Dt) = \nabla\cdot(\lambda\,\nabla T),$$

where Dh/Dt is the total time derivative of the enthalpy. For steady-state conditions, this equation may be written

$$\rho\underline{u}\cdot\nabla h = \nabla\cdot(\lambda\,\nabla T),$$

where $\underline{u}$ is the vector velocity. For the present case, with spherical symmetry, this equation may be integrated and expressed in the following form,

---

* In this formulation no explicit use is made of the momentum equation. It is shown in Appendix A that the condition for conservation of momentum reduces to the statement that the pressure is practically constant, which is assumed to be the case in the analysis.

$$[4\pi r^2 \rho\, uh]_1 - [4\pi r^2 \rho\, uh]_2 = -\left\{[4\pi r^2 \lambda (dT/dr)]_2 - [4\pi r^2 \lambda\, (dT/dr)]_1\right\} . \tag{2}$$

The terms $[4\pi r^2 \rho\, uh]_x$ represent the total enthalpy transport across the surface x; the subscripts 1 and 2 identify, respectively, the surfaces at r_1 and r_2.

The general continuity equation for species K can be written in the form*

$$\dot{m}_K = 4\pi r^2 \rho\, Y_K \left[(\dot{m}_F / 4\pi r^2 \rho\,) - (D_K / Y_K)\, (dY_K/dr)\right] \tag{3}$$

where $\dot{m}_K$ is the rate of mass transport of species K, ρ is the density of the gas mixture, Y_K equals the weight fraction of species K, and D_K is the appropriate diffusion coefficient for species K. Equation (3) states that the total mass transport of species K is equal to the sum of the mass transport of species K associated with the movement of the average fluid, $Y_K \dot{m}_F$, and with mass transfer by diffusion, $- 4\pi r^2 \rho\, D_K (dY_K/dr)$.

A. Derivation of Godsave's[7] Equation for $\dot{m}_F$.

In order to obtain Equation (1), which is the equation for droplet burning rates derived by Godsave, the expression for conservation of energy given in Eq. (2) is applied to the spherical shell between r_ℓ

---

* See Appendix B.

and r for $r < r_c$. The rate of enthalpy transport at r_ℓ is

$$\dot{m}_F (h_F)_{T_\ell} ,$$

and at r,

$$\dot{m}_F (h_F)_T .$$

The rate of energy transport by thermal conduction at r_ℓ is

$$- \left[4\pi r^2 \lambda \, (dT/dr) \right]_{r_\ell} = - \dot{m}_F \Delta\ell$$

and the rate of energy transport at r into the shell between r_ℓ and r is

$$4\pi r^2 \lambda \, (dT/dr) .$$

Hence Equation (2) becomes

$$\dot{m}_F \left[(h_F)_T - (h_F)_{T_\ell} \right] = - \dot{m}_F \, \Delta\ell + 4\pi r^2 \lambda \, (dT/dr)$$

or

$$4\pi r^2 (dT/dr) = (\dot{m}_F/\lambda) \left[\Delta\ell + \int_{T_\ell}^{T} (c_p)_F \, dT \right], \qquad (4)$$

where the subscript F to the specific heat identifies the fuel vapor. If it is assumed that λ is independent of temperature and also that $(c_p)_F$ is constant, then Equation (4) becomes

$$4\pi r^2 (dT/dr) = \left[\dot{m}_F (c_p)_F / \lambda \right] \left\{ \left[\Delta\ell / (c_p)_F \right] + (T - T_\ell) \right\}.$$

Integration of the preceding expression between the limits $r = r_\ell$ at $T = T_\ell$ and $r = r_c$ at $T = T_c$ leads directly to Godsave's equation for $\dot{m}_F$, viz.,

$$\dot{m}_F = \frac{4\pi\lambda}{(c_p)_F} \frac{\ln\left\{1 + \left[(c_p)_F (T_c - T_\ell)/\Delta\ell\right]\right\}}{\left[(1/r_\ell) - (1/r_c)\right]} \quad . \tag{5}$$

Reference to Equation (5), which is equivalent to Equation (1), shows that for $r_c \gg r$, or for constant values of r_ℓ / r_c, $\dot{m}_F$ is a linear function of the droplet radius. Furthermore, since T_c is generally large compared to T_ℓ, it follows that $\dot{m}_F$ is not a sensitive function of T_ℓ.

It should be noted that Equation (5) was derived without making any special assumptions about the location of the reaction front. For this reason the expression for $\dot{m}_F$ contains two unknown parameters, viz., T_c and r_c. Godsave measured* r_c, and found that the ratio of r_c to r_ℓ was a constant, and showed that for reasonable, assumed values of T_c, an acceptable correlation for the measured values of $\dot{m}_F$ was provided by Equation (5).

B. An Expression for $\dot{m}_F$ if λ and $(c_p)_F$ are Linear Functions of the Temperature

A refinement of Godsave's equation can be obtained without difficulty by deleting the assumptions that λ can be assigned an average value in the temperature interval between T_ℓ and T_c, and

---

* The experimental determination of r_c was greatly complicated by the fact that the combustion surface was far from spherical because of severe convection currents over the droplet.

that the specific heat of the fuel vapor is constant. The following approximate expression, which provides good agreement with experimental values, is used for the thermal conductivity:

$$\lambda = \lambda_\ell (T/T_\ell), \tag{6}$$

where λ_ℓ is the thermal conductivity of the fuel-inert gas mixture at the temperature T_ℓ. For the specific heat of the fuel vapor, the expression

$$(c_p)_F = a + bT, \tag{7}$$

is used, where a and b are constants chosen to give best fit with experimental data for $(c_p)_F$. Equations (4), (6), and (7) lead to the result

$$4\pi r^2 (dT/dr) = (\dot{m}_F T_\ell / \lambda_\ell T)\left[a(T - T_\ell) + (b/2)(T^2 - T_\ell{}^2) + \Delta\ell \right]. \tag{4a}$$

Integration of the preceding expression from r_ℓ, T_ℓ to r_c, T_c shows that

$$\dot{m}_F = \frac{4\pi \lambda_\ell r_\ell}{bT_\ell \left[1 - (r_\ell / r_c)\right]} \left[\ln \left\{ 1 + \left[(T_c - T_\ell)/\Delta\ell \right] \left[a + (b/2)(T_c + T_\ell) \right] \right\} \right.$$

$$\left. - \frac{a}{\xi} \ln \frac{(a + bT_c - \xi)(a + bT_\ell + \xi)}{(a + bT_c + \xi)(a + bT_\ell - \xi)} \right] \tag{8}$$

where

$$\xi = \left\{ a^2 - 2b\left[\Delta\ell - (b/2)T_\ell{}^2 - aT_\ell \right] \right\}^{1/2}. \tag{9}$$

It may be shown that this expression reduces to the expression computed for the case of constant specific heat when the limit is taken as b tends to zero.

Reference to Equations (8) and (9) shows again that $\dot{m}_F$ is determined provided r_c and T_c are known. We shall show in paragraphs IID and IIE that both T_c and r_c can be calculated by appropriate application of Equations (2) and (3) by utilizing the assumption that the delivery ratio of fuel to oxygen at the reaction front corresponds to the stoichiometric mixture ratio. Numerical calculation reveals that the value of the surface temperature, T_ℓ, exerts little influence on the value of $\dot{m}_F$ when varied within reasonable limits. Therefore T_ℓ may be set equal to the boiling temperature of the liquid.

C. Preliminary Remarks on the Use of Equations (2) and (3).

One of the objectives of the present analysis is to establish an efficient method for the utilization of the basic relations given in Equations (2) and (3). It will be convenient to restrict the analysis to spherical shells with $r_\ell < r < r_c$, or for $r_c < r < \infty$. In this case, simple explicit expressions are obtained for the rate of energy transport by thermal conduction through the surface of radius r. Thus Equation (2) leads to an expression of the form

$$4\pi r^2 \lambda \, (dT/dr) = \dot{m}_F (c_p)_K (\alpha + \beta T + \epsilon T^2) \qquad (10)$$

if the specific heat is a linear function of the temperature. Here the numerical values of α, β, and ϵ must be determined for each

particular problem. Equation (3) becomes

$$4\pi r^2 \rho D_K (dY_K/dr) = \dot{m}_F (Y_K - \gamma_K) \tag{11}$$

where

$$\gamma_K = \dot{m}_K/\dot{m}_F . \tag{12}$$

In the use of Equations (11) and (12), care must be taken to employ a positive value for γ_K if mass flow occurs in the same direction as the fuel transport, and to use a negative value for γ_K if mass flow occurs in the direction opposite to the direction of fuel transport.

It is evident by reference to Equations (10) and (11) that we can eliminate the radial distance as independent variable and write

$$\frac{dY_K}{Y_K - \gamma_K} = \chi_K \frac{dT}{\alpha + \beta T + \epsilon T^2} \tag{13}$$

where the dimensionless parameter χ_K, which has been called the Lewis Number by some investigators, is not a sensitive function of pressure and temperature, and is defined by the relation

$$\chi_K = \lambda/\rho D_K (c_p)_K . \tag{14}$$

It is further assumed that the parameter χ_K is independent of variations in Y_K.

Before discussing the integration of these equations, the boundary conditions appropriate to the burning drop problem should be considered. Far from the drop, as r tends to infinity, the gas tempera-

ture and oxidizer weight fraction become the ambient values, T_o and $Y_{O,o}$ respectively. At the flame front, the temperature is T_c, and is evaluated by use of the procedure outlined in the following paragraph. The concentrations of fuel vapor and oxidizer, Y_F and Y_O respectively, are equal to zero at the flame front. This condition arises from the assumption that the rates of mass diffusion are much lower than the chemical reaction rates. Hence, the chemical reaction is capable of using more reactant than can be delivered by the transport processes. For the purposes of analysis, the reaction rate is taken to be infinite, i.e., the reactants are consumed instantaneously upon reaching the flame front, and the reactant concentration there is equal to zero. The temperature at the drop surface is T_ℓ , a value less than or equal to the normal boiling temperature. The fuel vapor weight fraction there is $Y_{F,\ell}$, a value between zero and unity. For equilibrium conditions, $Y_{F,\ell}$ and T_ℓ would be interrelated through the vapor pressure - temperature relation for the fuel. In the present non-equilibrium case, the vapor pressure-temperature relation does not hold exactly, but might be used as an approximation. It has been seen, however, that the exact value for the drop surface temperature exerts little influence on the calculated burning rate, hence could be set equal to the normal boiling temperature for the purposes of numerical calculation. This would imply that the value of $Y_{F,\ell}$ is equal to one.

Integration of Equation (13) between $Y_O = 0$ at $r = r_c$ and $Y_O = Y_{O,o}$ at $r = \infty$, corresponding to T_c and T_o, respectively, leads directly to the value of T_c for specified values of T_o and

$Y_{O,o}$.* A mean value of $(c_p)_K$ is assumed. The parameters λ, ρ, and D may be evaluated at any convenient temperature. Similarly, integration between $Y_F = Y_{F,\ell}$ at $r = r_\ell$, $T = T_\ell$ and $Y_F = 0$ at $r = r_c$, $T = T_c$, gives an explicit expression for $Y_{F,\ell} = 1 - Y_{I,\ell}$.**

In order to obtain the value of r_c we can utilize Equation (10) or Equation (11). Equation (10) can be integrated directly between r_c, T_c and ∞, T_o, after expressing λ as a linear function of T. Introduction of the known relation for $\dot{m}_F$ into the resulting expression leads to an explicit relation for r_c. The integration of Equation (11) is somewhat more involved since ρD_K is a linear function of T to the same approximation that λ is a linear function of T. Hence integration of Equation (11) requires the determination of T(r) prior to integration. We shall use Equation (10) for the determination of r_c.

By utilizing constant average specific heats only in the region $r \geq r_c$, it is to be expected that reasonable estimates, commensurate in accuracy with our assumed physical model, will be obtained for T_c, r_c, and $\dot{m}_F$. Examination of experimental data[22] for specific heats reveals that the variation in c_p with temperature is not large for the

---

* The same result is obtained if we integrate Equation (12) from $Y_I = 1$ at $r = r_c$, $T = T_c$ to $Y_I = 1 - Y_{0,o}$ at $r = \infty$, $T = T_o$.

** The same result is obtained if we integrate Equation (12) from $Y_{I,\ell}$ at $r = r_\ell$, $T = T_\ell$ to $Y_I = 1$ at $r = r_c$, $T = T_c$.

temperature range of interest here for the species O_2, N_2, H_2O, and CO_2. This is in contrast to the behavior of the specific heats of hydrocarbon vapors, which show large variations with temperature.

D. Determination of T_c and of $Y_{F,\ell}$.

(1) The Reaction Zone Temperature T_c.

For the spherical shell between $r \searrow r_c$ and r_c, Equation (2) becomes

$$\dot{m}_F \left[(1 + \gamma_O)(h_P)_T - \gamma_O(h_O)_T\right] - \dot{m}_F\left[(1 + \gamma_O)(h_P)_{T_c} - \gamma_O(h_O)_{T_c}\right]$$

$$= 4\pi r^2\lambda(dT/dr) - \left[4\pi r^2\lambda(dT/dr)\right]_{r_c}, \qquad (15)$$

where h_P and h_O denote, respectively, the specific enthalpies of products of reaction and of oxidizer. But $-\left[4\pi r^2\lambda\,(dT/dr)\right]_{r_c}$ equals the total heat evolved on reaction at T_c minus the energy transported to the fuel droplet, i.e.,

$$-\left[4\pi r^2\lambda\,(dT/dr)\right]_{r_c} =$$

$$\dot{m}_F\left\{\left[-(1 + \gamma_O)(h_P)_{T_c} + (h_F)_{T_c} + \gamma_O(h_O)_{T_c}\right] - \Delta\ell - \left[(h_F)_{T_c} - (h_F)_{T_\ell}\right]\right\}$$

where h_F is the specific enthalpy of the fuel vapor. Hence Equation (15) becomes

$$-4\pi r^2\lambda(dT/dr) = \dot{m}_F\left\{q^* + \gamma_O\left[(h_O)_T - (h_O)_{T^*}\right] - (1 + \gamma_O)\left[(h_P)_T - (h_P)_{T^*}\right]\right\}, \qquad (16)$$

where

$$q^* = -(1 + \gamma_O)(h_P)_{T^*} + (h_{F,\ell})_{T^*} + \gamma_O (h_O)_{T^*} + c_\ell (T_\ell - T^*). * \qquad (17)$$

Here T^* is a standard reference temperature (usually chosen as $298.16^\circ K$) and c_ℓ denotes a constant specific heat for the liquid fuel in the temperature range between T^* and T_ℓ ; the quantity q^* differs from the standard heat of reaction for one gram of liquid fuel and γ_O grams of gaseous oxidizer, both initially at temperature T^*, forming H_2O and CO_2 at a temperature of T^*, through the addition of the small term $c_\ell (T_\ell - T^*)$. If $(c_p)_P$ and $(c_p)_O$ are taken to be independent of the temperature, then Equation (16) reduces to the relation

$$4\pi r^2 \lambda (dT/dr) = \dot{m}_F \left\{ q^* + (T - T^*) \left[\gamma_O (c_p)_O - (1 + \gamma_O)(c_p)_P \right] \right\} . \qquad (16a)$$

Reference to Equation (16a) shows that it is of the form

---

* For the present approximate calculations the heat release q^* and, therefore, T_c, r_c/r_ℓ , and $\dot{m}_F$ are computed by neglecting the effect of dissociation of combustion products, fuel, and oxygen. The derived results would be expected to be roughly correct for gas mixtures leading to values of T_c well below $3000^\circ K$, i.e., for some hydrocarbon-air flames. The effect of dissociation on the calculated results can be incorporated into our present model by using an iteration procedure in which it is assumed that chemical equilibrium is established at every point. As the result of this refinement, the calculated values of T_c and r_c/r_ℓ are decreased by a first iteration; the temperature profile toward the oxidizer is flattened and the temperature raised because the reassociating gases act as a distributed heat source on recombination. The diffusive flow of oxygen inward is then increased, thereby leading to a further decrease of r_c/r_ℓ . Rough calculations show that the net effect of dissociation on the calculated values of $\dot{m}_F$ for benzene-air flames is probably less than 10 $^o/o$ although both T_c and r_c/r_ℓ are decreased appreciably.

$$4\pi r^2 \lambda \, (dT/dr) = \dot{m}_F \, (c_p)_O \, (\alpha + \beta T) \tag{16b}$$

with

$$\alpha = - \left[q^*/(c_p)_O \right] - \beta T^* \tag{18}$$

and

$$\beta = (1 + \gamma_O) \, \delta_P - \gamma_O \, , \tag{19}$$

where $\delta_K = (c_p)_K/(c_p)_O$.

From Equation (11) we can obtain the appropriate expression for the mass transfer of oxidizer,

$$4\pi r^2 \rho \, D_O \, (dY_O/dr) = \dot{m}_F \, (Y_O + \gamma_O) \, , \tag{20}$$

where a negative sign has been used for γ_O because the oxidizer flows in a direction opposite to that of the fuel. Here D_O is the diffusion coefficient of oxidizer through the oxidizer-inert gas-combustion products mixture. Division of Equation (16b) by Equation (20) leads to the expression

$$\frac{dY_O}{Y_O + \gamma_O} = \frac{dT}{\alpha + \beta T} \, \chi_O \tag{21}$$

where

$$\chi_O = \lambda/(c_p)_O D_O \rho$$

is a constant. Hence integration of Equation (21) between $Y_O = 0$, $T = T_c$ and $Y_O = Y_{O,o}$, T_o leads to the following explicit relation for T_c:

$$T_c = \frac{\beta T_o - \alpha\left\{\left[1 + (Y_{O,o}/\nu_O)\right]^{(\beta/\chi_O)} - 1\right\}}{\beta\left[1 + Y_{O,o}/\nu_O\right]^{(\beta/\chi_O)}} \quad . \tag{22}$$

(2) The Weight Fraction Profile of Fuel Vapor.

It is evident from the formulation of the present problem that Y_F cannot equal unity at the droplet surface. For this reason it is of interest to estimate Y_F at r_ℓ approximately.

From Equation (3a) and Equation (10), written in terms of the fuel, it follows that

$$\frac{dY_F}{Y_F - 1} = \frac{\lambda}{\rho D_F} \frac{dT}{(b/2)T^2 + aT + \left[\Delta\ell - aT_\ell - (b/2)T_\ell^2\right]} \tag{23}$$

where $\lambda/\rho D_F$ is independent of temperature and is assumed to be independent of Y_F. Integration of Equation (23) between $Y_F = Y_{F,\ell}$ at $T = T_\ell$ and $Y_F = 0$ at $T = T_c$ leads to the result

$$Y_{F,\ell} = 1 - \left[\frac{(a + bT_c - \xi)(a + bT_\ell + \xi)}{(a + bT_c + \xi)(a + bT_\ell - \xi)}\right]^{-(\lambda/\rho D_F \xi)} \tag{24}$$

where ξ has been defined in Equation (9).

E. Determination of the Combustion Radius

Equation (16b), which was derived on the assumption that the specific heats of oxidizer and inert gas are constant for $r \geq r_c$, may be used directly for the determination of r_c. After replacing λ by

$\lambda_\ell\ (T/T_\ell\ )$ and integrating from r_c, T_c to ∞, T_o, the following relation is obtained:

$$\frac{1}{r_c} = \frac{4\pi\lambda_\ell}{\dot{m}_F (c_p)_o T_\ell} \left[\frac{1}{\beta} (T_o - T_c) - \frac{\alpha}{\beta^2} \ln \frac{\alpha + \beta T_o}{\alpha + \beta T_c} \right] \tag{25}$$

where α and β are defined in Equations (17) and (18), respectively.

From Equations (8) and (25) we can now obtain an explicit expression for r_c/r_ℓ. Thus we may write Equation (8) in the form

$$\dot{m}_F = \frac{4\pi\lambda_\ell r_\ell}{bT_\ell \left[1 - r_\ell/r_c\right]} \psi \quad , \tag{8a}$$

where

$$\psi = \ln \left\{ 1 + \left[(T_c - T_\ell)/\Delta\ell \right] \left[a + (b/2)(T_c + T_\ell) \right] \right\} - \frac{a}{\xi} \ln \frac{(a + bT_c - \xi)(a + bT_\ell + \xi)}{(a + bT_c + \xi)(a + bT_\ell - \xi)} \quad . \tag{26}$$

From Equations (25) and (8a) it is seen that

$$\frac{r_c}{r_\ell} = 1 + \frac{(c_p)_o \psi}{b} \left[\frac{1}{\beta} (T_o - T_c) - \frac{\alpha}{\beta^2} \ln \frac{\alpha + \beta T_o}{\alpha + \beta T_c} \right]^{-1} \tag{27}$$

Reference to Equation (27) shows the interesting result, which is in accord with some of the experimental observations, that r_c/r_ℓ is a constant for fixed values of the physico-chemical parameters. Hence Equation (8a) shows that $\dot{m}_F$ is a linear function of r_ℓ.

The linear function relation between $\dot{m}_F$ and r_ℓ has been used by Godsave[7] to obtain the following expression for the variation

of droplet diameter with time:

$$d^2 = d_0^2 - K't \,. \tag{28}$$

Here d is the droplet diameter at time t, d_0 is the initial droplet diameter, and the evaporation constant K' is defined by the relation

$$K' = 2\dot{m}_F/\pi r_\ell \rho_\ell = 8 \lambda_\ell \Psi / \rho_\ell \, bT_\ell \left[1 - r_\ell / r_c\right]. \tag{29}$$

Since K' is independent of r_ℓ, it is a convenient parameter for comparing burning rates of different fuels for arbitrary droplet sizes.

The results of calculations for the burning of benzene, ethyl alcohol, n-heptane, and toluene in air are summarized in Table I. Also listed in Table I are appropriate values of the physico-chemical parameters.

For the sake of completeness, T vs. r and Y_K vs. r profiles have been determined for the burning of a benzene droplet in air for $T_o = 300^oK$ and $r_\ell = 0.005$ cm. The results of these calculations have been considered previously and are given in Figures 3a to 3d. Comparisons of the theoretical results to experimental data will be carried out in Section V.

TABLE I. PHYSICO-CHEMICAL PARAMETERS AND CALCULATED VALUES FOR THE BURNING OF DROPS OF BENZENE, ETHYL ALCOHOL, ETHYL BENZENE, N-HEPTANE, AND TOLUENE IN AIR AT ATMOSPHERIC PRESSURE.

Fuel	T_o ($^\circ K$)	$Y_{O,o}$	Y_o	T_ℓ ($^\circ K$)	ρ_ℓ ($\frac{gm}{cm^3}$)	$\Delta\ell$ ($\frac{cal}{gm}$)	a ($\frac{cal}{gm-^\circ K}$)	b ($\frac{cal}{gm-(^\circ K)^2}$)	λ_ℓ ($\frac{cal}{cm-Sec-^\circ K}$)	χ_o
Benzene	300	0.23	3.08	353	0.84	94.0	0.34	0.25×10^{-3}	55×16^{-6}	0.77
Ethyl Alcohol	300	0.23	2.09	351	0.79	204	0.44	0.26×10^{-3}	55×10^{-6}	0.77
n-Heptane	300	0.23	3.52	371	0.68	75.6	0.44	0.40×10^{-3}	55×10^{-6}	0.77
Toluene	300	0.23	3.13	384	0.84	87.0	0.37	0.25×10^{-3}	55×10^{-6}	0.77

Fuel	$(C_p)_O$ ($\frac{cal}{gm-^\circ K}$)	δ_p	T^* ($^\circ K$)	q^* ($\frac{cal}{gm}$)	β	α ($^\circ K$)	T_c^* ($^\circ K$)	ξ ($\frac{cal}{gm-^\circ K}$)	ψ	r_c/r_ℓ^*	K'^* ($\frac{cm^2}{sec}$)
Benzene	0.26	1.35	298	9790	2.43	-38,375	3450	0.37	1.51	9.6	10.0×10^{-3}
Ethyl Alcohol	0.26	1.58	298	6460	2.79	-25,680	3100	0.42	1.05	5.3	7.9×10^{-3}
n-Heptane	0.26	1.58	298	10625	3.63	-42,180	3230	0.54	1.75	8.6	8.6×10^{-3}
Toluene	0.26	1.39	298	9750	2.61	-38,300	3370	0.42	1.43	9.5	8.7×10^{-3}

* See footnote on page 19 for a discussion of the effect of dissociation on T_c and on r_c/r_ℓ. For benzene T_c is decreased from 3450°K to about 2600°K when proper allowance is made for dissociation. However, the effect of corrections for dissociation on K' is probably small.

III. THERMAL THEORY FOR DROPLET BURNING

In the preceding section, a theory for the burning of fuel droplets was presented which assumes that the chemical reaction rates are infinitely high, and that the diffusion of the reactants is the overall rate-determining factor. In contrast to that diffusion theory, in this section a theory for droplet burning will be presented in which it is assumed that the diffusion and mixing of the reactants occur very rapidly, and that the chemical reaction rates determine the overall rate of burning of the drop. This theory has been motivated by the desire to have a theory that is simpler in form than the previous diffusion theory, yet adequate to explain the observed characteristics of droplet combustion. The ultimate goal of the calculation would be to use this simpler theory as a basis for extention to the case of a droplet burning under conditions of forced convection. It was felt that the thermal theory, using as it does only the heat transfer equation, would be more amenable for such a calculation than the diffusion theory, which requires simultaneous consideration of the heat and mass transfer equations.

For the purposes of analysis, a steady-state, spherically symmetric model will again be used. In this theory, however, the flame zone surrounding the droplet is assumed to have finite thickness. This thickness is assumed to be small in comparison to the drop size. A diagram of this model is shown in Figure 4. As before, the droplet radius is r_ℓ, but the radial distance to the inside surface of the flame zone is now called r_i. Except as otherwise noted, all notation will be similar to that used in the diffusion theory.

The physical assumption of this theory is that the oxidizer from the surrounding atmosphere diffuses inward rapidly and mixes with the fuel vapor being evaporated from the drop surface. The reactants are then burnt as a homogeneous mixture. With this assumption, the model of the burning process for the case of a fuel droplet surrounded by an oxidizing atmosphere is identical to the case of a monopropellant drop burning in an inert atmosphere. This physical model was first suggested by Kuo[19].

For purposes of analysis, it is assumed that the overall chemical reaction rate can be described by the so-called zero-order kinetics, in which the reaction rate is independent of reactant concentration. An Arrhenius type reaction rate law is assumed, hence the reaction rate is strongly temperature dependent. Similar assumptions have been made by Semenov[20] and others treating the pre-mixed laminar flame propagation problem. Such theories are usually called "thermal theories", hence the same title has been given to the present analysis.

With the above assumptions, it is no longer necessary to consider the equations of diffusion of mass; only the equations of temperature distribution must be dealt with. As may be seen from the schematic temperature profile shown in Figure 4, the region surrounding the droplet may be conveniently divided into three zones. First there is the zone between the droplet and the combustion zone, $r_\ell < r < r_i$. The temperature T_i at the inside of the combustion zone is called the ignition temperature, and it is assumed that no reaction takes place until this temperature is reached. In the thin combustion zone, $r_i < r < r_{i'}$,

the temperature increases from T_i to the peak temperature, T_p, and then decreases again to the value $T_{i'}$ at the outside edge, where the reaction is assumed to be completed. Outside the reaction zone, $r \geq r_{i'}$, the temperature decreases from $T_{i'}$ to the temperature of the surrounding infinite medium, T_o.

A. Calculation of Burning Rate

In this analysis, mean values will be used for the physical parameters. The appropriate differential equation for the steady-state temperature distribution may then be written in vector notation as

$$\lambda \nabla^2 T - c_p \rho \bar{V} \cdot \nabla T + \rho Q = 0, \qquad (30)$$

where λ, c_p, and ρ are the thermal conductivity, specific heat at constant pressure, and density, respectively. The convection velocity is $\bar{V}$ and Q is the rate of heat generation resulting from chemical reaction per unit mass of gas. For this spherically symmetric system, the equation may be simplified to read,

$$d^2T/dr^2 + \left[2/r - (c_p \rho/\lambda)(\dot{m}_F/4\pi r^2 \rho) \right] (dT/dr) + \rho Q/\lambda = 0. \qquad (30a)$$

This equation will be solved separately for the three regions outside the drop surface, and the solutions will be joined by requiring that the values for the temperature and its first derivative be continuous throughout.

First, this equation will be integrated to obtain the temperature profile in the innermost zone, between the drop surface and the inside of the flame. In this region Q is equal to zero, as it has been assumed

that no reaction takes place at a temperature below T_i. The boundary conditions are $T = T_i$ at $r = r_i$ and $T = T_\ell$ at $r = r_\ell$. The temperature at the drop surface, T_ℓ, is assumed to be equal to the normal boiling temperature of the liquid fuel. The expression for the temperature is found to be

$$T = \frac{(T_i - T_\ell)\exp\left[-(\Lambda/r)\right] + T_\ell \exp\left[-(\Lambda/r_i)\right] - T_i \exp\left[-(\Lambda/r_\ell)\right]}{\exp\left[-(\Lambda/r_i)\right] - \exp\left[-(\Lambda/r_\ell)\right]} \tag{31}$$

where

$$\Lambda = c_p \dot{m}_F / 4\pi\lambda \tag{32}$$

The requirement must now be met that the heat conducted to the droplet be equal to the heat necessary to evaporate the liquid fuel, or

$$4\pi\lambda r_\ell^2 \left(dT/dr\right)\Big|_{r_\ell} = \dot{m}_F \Delta\ell. \tag{33}$$

Differentiating Equation (31) gives

$$(dT/dr) = \frac{(T_i - T_\ell)\dot{m}_F c_p}{4\pi\lambda r^2} \cdot \frac{\exp(-\Lambda/r)}{\exp(-\Lambda/r_i) - \exp(-\Lambda/r_\ell)}, \tag{34}$$

and substituting this equation into Equation (33) gives

$$\Delta\ell = (T_i - T_\ell)\, c_p / \left\{\exp\left[\Lambda\,(1/r_\ell - 1/r_i)\right] - 1\right\}. \tag{35}$$

Rearranging this equation yields the following expression for $\dot{m}_F$:

$$\dot{m}_F = \left[4\pi\lambda r_\ell / c_p (1 - r_\ell / r_i)\right] \ln \left[1 + c_p (T_i - T_\ell)/\Delta\ell\right] . \qquad (35a)$$

This result is similar to that of Godsave (i.e., Equation (1)).

Next, Equation (30a) must be integrated in the flame region, $r_i < r < r_{i'}$. The rate of heat release, Q, is expressed in the following form:

$$Q = \mathcal{R} H \phi \exp(-E/RT), \qquad (36)$$

where R is the universal gas constant, E is the activation energy for the reaction, ϕ is the frequency factor, H is the heat released from the complete burning of unit mass of fuel, and $\mathcal{R}$ is the weight fraction of fuel present in the fuel-oxidizer-inert gas mixture. Henceforth, the ratio E/R will be denoted by $\overline{T}$ and called the "characteristic temperature". The temperature distribution equation then becomes

$$d^2T/dr^2 + [2/r - c_p \dot{m}_F/4\pi r^2\lambda](dT/dr) + (\rho \mathcal{R} H \phi/\lambda) \exp(-\overline{T}/T) = 0 . \qquad (37)$$

As an exact solution to this complete equation could not be found, a simplifying approximation has been made. In the thin flame zone, it is assumed that the temperature gradient is small in comparison to the rate of change of gradient, i.e., the factor dT/dr is small in comparison to d^2T/dr^2. Dropping this term in Equation (37) means that the rate of transport of heat is small in comparison to the rate of heat release due to combustion. Equation (37) may then be written,

$$d^2T/dr^2 + (\rho \mathcal{R} \phi H/\lambda) \exp(-\overline{T}/T) = 0. \qquad (38)$$

To integrate this equation, let

$$(dT/dr) = \eta \ .$$

Then Equation (38) may be written

$$\eta \, (d\eta/dT) = - (\varrho \mathcal{R} \phi \ H/\lambda) \exp (-\bar{T}/T)$$

or

$$\eta \, d\eta = - (\varrho \mathcal{R} \phi \ H/\lambda) \exp (-\bar{T}/T) \, dT \ . \qquad (39)$$

If the not unreasonable assumption is made that the frequency factor is proportional to the absolute temperature, the term $(\varrho \ H \mathcal{R} \phi/\lambda)$ is temperature-independent, and Equation (39) may be integrated to yield

$$(1/2)\eta^2 = - (\varrho \ H \mathcal{R} \phi \ /\lambda) \int \exp (-\bar{T}/T) dT + C$$

where C is the constant of integration. The exponential term in the above integrand could be expanded into a series, then integrated term by term; this results, however, in an unwieldy series in which many terms must be retained in order to obtain acceptable accuracy. A better method is to obtain an a symptotic expansion for the integral. Making the substitution $\bar{T}/T = \Upsilon$, and integrating by parts yields the following expression,

$$\int \exp (-\bar{T}/T) dT = \left[\bar{T} \exp (-\Upsilon) \right] \left[\ 1/\Upsilon \right] \Big\{ 1 - 2/\Upsilon + 6/\Upsilon^2$$

$$-24/\Upsilon^3 \ \cdots\cdots \ (-)^n \, (n+1)! \, /\Upsilon^n \ \cdots \Big\} \ . \qquad (40)$$

As Υ is generally greater than 8 or so, acceptable accuracy is obtained by using only the first term of the series. Hence

$$\int \exp (-\bar{T}/T) dT \simeq \quad (T^2/\bar{T}) \exp (-\bar{T}/T) \ , \qquad (41)$$

and

$$(1/2)\eta^2 = C - (\rho H \mathcal{R} \phi / \lambda)(T^2/\bar{T}) \exp(-\bar{T}/T). \qquad (42)$$

The value of the constant, C, is obtained by applying the condition that dT/dr, i.e., η, is equal to zero at the position of peak temperature, $T = T_p$. Therefore,

$$C = (\rho H \mathcal{R} \phi / \lambda)(T_p^2/\bar{T}) \exp(-\bar{T}/T_p)$$

and

$$\eta = \pm (2\rho H \mathcal{R} \phi / \lambda)^{1/2} \left\{ (T_p^2/\bar{T}) \exp(-\bar{T}/T_p) - (T^2/\bar{T}) \exp(-\bar{T}/T) \right\}^{1/2} \qquad (43)$$

The positive sign is used for η when $r < r_p$ and the negative sign is used for $r > r_p$.

As the ignition temperature, T_i, is considered to be several hundred degrees below the peak flame temperature, T_p, the second term on the right hand side of Equation (43) may be ignored when $T = T_i$, and the following expression for the temperature gradient at $r = r_i$ is obtained:

$$(dT/dr)\Big|_{r = r_i} = (2\rho H \mathcal{R} \phi / \lambda \bar{T})^{1/2} T_p \exp(-\bar{T}/2T_p). \qquad (44)$$

Similar reasoning gives the value of the temperature derivative at the outside boundary of the flame zone, $r = r_{i'}$.

$$(dT/dr)\Big|_{r = r_{i'}} = -(2\rho H \mathcal{R} \phi / \lambda \bar{T})^{1/2} T_p \exp(-\bar{T}/2T_p). \qquad (45)$$

It is seen that the physical assumptions used in integrating the tempera-

ture equation through the flame zone lead to a temperature profile in this region that is symmetrical about the peak temperature, T_p.

The next step in the analysis is to integrate Equation (30a) in the region outside the flame zone, i.e., for $r > r_{i'}$. As was done for the case of the region inside the flame zone, Q will be set equal to zero, as it is assumed that no reaction takes place outside the thin flame region. Equation (30a) may then be integrated at once to obtain

$$T = \frac{(T_o - T_{i'}) \exp(-\Lambda/r) + T_{i'} - T_o \exp(-\Lambda/r_{i'})}{1 - \exp(-\Lambda/r_{i'})} \tag{46}$$

and

$$dT/dr = \frac{(T_o - T_{i'}) \dot{m}_F c_p \exp(-\Lambda/r)}{\left[1 - \exp(-\Lambda/r_{i'})\right] 4\pi r^2 \lambda} \tag{47}$$

This solution is subject to the condition that the heat lost by conduction to the surrounding medium must be equal to the heat released by combustion of the fuel vapor minus the heat necessary to evaporate the liquid fuel, or, as $r \to \infty$,

$$-4\pi r^2 \lambda \, (dT/dr)\Big|_{r \to \infty} = \dot{m}_F \left[H - \Delta \ell \right]. \tag{48}$$

Therefore

$$(T_{i'} - T_o) c_p / \left[1 - \exp(-\Lambda/r_{i'}) \right] = H - \Delta \ell \ . \tag{49}$$

As has been stated before, it is required that the solutions of the temperature equation in the three separate regions be joined so that no discontinuities in the temperature or the first derivative occur at the boundaries of the regions. Therefore

$$(dT/dr)\Big|_{r = r_i\,(r \searrow r_i)} = (dT/dr)\Big|_{r = r_i\,(r \swarrow r_i)} .$$

Substituting from Equations (34), (35), and (44),

$$(2\mathcal{R} H \varsigma\phi/\lambda\bar{T})^{1/2}\, T_p \exp(-\bar{T}/2T_p) = (\dot{m}_F \Delta\ell/4\pi\lambda r_i^2)\left[1 + (c_p/\Delta\ell)(T_i - T_\ell)\right]. \quad (50)$$

Also

$$(dT/dr)\Big|_{r = r_{i'}\,(r \swarrow r_{i'})} = (dT/dr)\Big|_{r = r_{i'}\,(r \searrow r_{i'})},$$

and from Equations (45), (47), and (49),

$$(2\varsigma H\mathcal{R}\phi/\lambda\bar{T})^{1/2}\, T_p \exp(-\bar{T}/2T_p) = \dot{m}_F (H - \Delta\ell) \exp(-\Lambda/r_{i'})/4\pi\lambda r_{i'}^2 . \quad (51)$$

As the left-hand sides of Equations (50) and (51) are identical, the right-hand sides can be equated to yield

$$(H - \Delta\ell) \exp(-\Lambda/r_{i'}) r_i^2 = \Delta\ell \left[1 + (c_p/\Delta\ell)(T_i - T_\ell)\right] r_{i'}^2. \quad (52)$$

In the above equation, $r_{i'}$ may be replaced by r_i, as the flame zone has been assumed to be thin and the ratio of $r_{i'}$ to r_i is nearly unity. Making this simplification in Equation (52) and utilizing Equation (35) gives

$$\exp(\Lambda/r_\ell) = \frac{H - \Delta\ell}{\Delta\ell} . \quad (53)$$

Taking the logarithm of both sides of this equation and rearranging terms yield the following expression for the mass burning rate of the

droplet in terms of known physico-chemical parameters:

$$\dot{m}_F = (4\pi\lambda r_\ell / c_p) \ell n \left[H/\Delta\ell - 1\right]. \qquad (54)$$

For most hydrocarbon fuels, the ratio $H/\Delta\ell$ is of the order 10^2, hence an adequate numerical approximation to Equation (54) is

$$\dot{m}_F = (4\pi\lambda r_\ell / c_p) \ell n (H/\Delta\ell). \qquad (54a)$$

In marked contrast to the results of the diffusion theory, this droplet burning rate as computed by the thermal theory is independent of the oxidizer concentration in the surrounding gas mixture. This result might be expected as a consequence of the simplified chemical rate law that is assumed.

B. Calculation of Flame Radius and Temperature

It has been shown in the previous paragraphs that the temperature profile within the flame as calculated by the present simplified theory is symmetric about the point of peak temperature. While no specific mention has been made of the value of the temperature at the outside of the combustion zone, $T_{i'}$, it is apparent from consideration of the exponential rate law, Equation (36), that, for the large values of activation energy, E , usually encountered, the chemical reaction has effectively ceased when the temperature has decreased to a value several hundred degrees below the peak flame temperature. Therefore, for the sake of simplicity, the value of $T_{i'}$ will be taken to be equal to the value of T_i, the ignition temperature. From these considerations and the fact that flame has been assumed to be thin, it is

apparent that the heat release within the flame must be distributed so that one-half of the total heat must be released inside the point of peak temperature and one-half outside of that point. Furthermore, the total heat released inside the point of peak temperature must be just the amount necessary to evaporate the liquid fuel and raise the vapor to the ignition temperature, T_i. Therefore the following important relation must be satisfied:

$$\Delta\ell + c_p(T_i - T_\ell) = H/2 . \tag{55}$$

The value of T_i may be obtained from this equation. If the values of H, $\Delta\ell$ and c_p of typical hydrocarbons are used, it is found that T_i is very large. These high calculated temperatures result from the fact that dissociation has been ignored.

It is now possible to calculate the value of the flame radius. First the expressions for drop burning rate given by Equations (35a) and (59) are equated and similar terms cancelled to obtain

$$\ell n\left[H/\Delta\ell - 1\right] = \frac{1}{1 - r_\ell/r_i}\ \ell n\left[1 + c_p(T_i - T_\ell)/\Delta\ell\right]. \tag{56}$$

Then, using the relation of Equation (55), Equation (56) may be solved to obtain the following explicit expression for the ratio r_ℓ/r_i.

$$r_\ell/r_i = 1 - \left\{\ell n\left[H/2\Delta\ell\right]/\ell n\left[H/\Delta\ell - 1\right]\right\} . \tag{57}$$

Here again, as in the diffusion theory, the calculated ratio of flame radius to drop radius is constant during the burning of the droplet.

To complete the calculations for this thermal theory, the value of T_p will be determined. From Equation (37),

$$(dT/dr)\Big|_{r = r_i} = (T_i - T_\ell)\, \dot{m}_F c_p / 4\pi\lambda r_i^2 \left\{1 - \exp\left[-\Lambda(1/r_\ell - 1/r_i)\right]\right\} . \tag{58}$$

From Equation (35),

$$\exp\left[\Lambda (1/r_\ell - 1/r_i)\right] = 1 + c_p (T_i - T_\ell)/\Delta\ell ;$$

therefore,

$$1 - \exp\left[-\Lambda(1/r_\ell - 1/r_i)\right] = (c_p/\Delta\ell)(T_i - T_\ell)/\left[1 + (c_p/\Delta\ell)(T_i - T_\ell)\right] .$$

Substitute this expression into Equation (58) and equate the resulting expression for $dT/dr\Big|_{r = r_i}$ to Equation (44). After cancelling and rearranging terms, the following expression for $\dot{m}_F$ is obtained:

$$\dot{m}_F = 4\pi\lambda r_i^2 (2\varsigma H\Re\phi/\lambda\bar{T})^{1/2} T_p \exp\left[-\bar{T}/2T_p\right]/\left[\Delta\ell + c_p (T_i - T_\ell)\right] . \tag{59}$$

This expression for the mass burning rate is then equated to the burning rate as expressed by Equation (59). Equations (55) and (57) are then used to eliminate the quantity r_i, and the following implicit expression for the temperature T_p is obtained:

$$T_p \exp(-\bar{T}/2T_p) = \frac{1}{r_\ell}\sqrt{\frac{\bar{T}\lambda H}{8\varsigma\phi\Re}}\left[1 - \frac{\ln(H/2\Delta\ell)}{\ln\{(H/\Delta\ell) - 1\}}\right]^2 \frac{\ln\left[H/\Delta\ell - 1\right]}{c_p} . \tag{60}$$

It is seen that T_p is a function of the drop radius, r_ℓ . As the drop decreases in size, the peak temperature, T_p, increases.

To recapitulate, the droplet burning rate may be quickly calculated from Equation (59). This equation predicts that the mass burning rate is proportional to the drop diameter, which agrees not only with the results of the previous diffusion theory, but also with experimental data. However, the thermal theory predicts no change of burning rate as oxidizer concentration or temperature are varied.

This very simple result arises directly from the assumptions leading to symmetry of the temperature profile in the thin flame zone and from the fact that the chemical reaction rate law assumed does not depend on reactant concentration. If a more accurate reaction rate law was used, so that the rate of chemical reaction was dependent on reactant concentration, and if the effects of mass diffusion were included in the theory, the calculated mass burning rate would be dependent on the oxidizer concentration. Because the results of this type of theory are sensitive to the form of chemical reaction rate law chosen, and because our knowledge of the kinetics of complex reactions is very limited, it is not to be expected that accurate results will be obtained from calculations of this sort.

C. A Simplified Thermal Theory

A much simpler scheme for the calculation of droplet burning rates has been considered. This method is based only on heat transfer considerations. The physical model of the diffusion theory is retained, with an infinitely thin spherical flame front surrounding the droplet.

It is then assumed that the flame temperature is equal to the adiabatic flame temperature for a stoichiometric mixture of the fuel and the surrounding oxidizer-inert gas atmosphere. The flame size is set by the requirement that the rate of heat conduction to the surrounding infinite atmosphere is equal to the rate of heat released by combustion minus the amount necessary to evaporate the liquid fuel.

The problem is easily formulated through use of the expression for conservation of energy given by Equation (2). For this calculation, a constant mean value of the specific heat will be used for the gases surrounding the droplet, and the thermal conductivity is assumed to be a linear function of the absolute temperature (see Equation (6)).

Equation (2) will first be applied to the spherical shell for $r_\ell < r < r_c$. Thus the rate of enthalpy transport at r minus that at r_ℓ may be written

$$\dot{m}_F c_p (T - T_\ell) .$$

The rate of energy transport by thermal conduction at r_ℓ is

$$-\left[4\pi r^2 \lambda (dT/dr)\right]_{r_\ell} = -\dot{m}_F \Delta\ell ,$$

hence Equation (2) becomes

$$\dot{m}_F \left[c_p (T - T_\ell) + \Delta\ell\right] = 4\pi r^2 \lambda_\ell (T/T_\ell)(dT/dr) . \qquad (61)$$

This equation may now be integrated between the limits r_ℓ , T_ℓ and r_c, T_c and rearranged to yield the following expression for the mass burning rate:

$$\dot{m}_F = \frac{4\pi \lambda_\ell r_\ell}{T_\ell c_p \left[1 - (r_\ell / r_c)\right]} \left\{ \left[T_\ell - (\Delta \ell / c_p) \right] \times \right.$$

$$\left. \ell n \left[1 + c_p (T_c - T_\ell)/\Delta \ell \right] + (T_c - T_\ell) \right\} \qquad (62)$$

In the same way, Equation (2) is applied to the region outside the combustion zone. Here, however,

$$- 4\pi \lambda r^2 (dT/dr) = \dot{m}_F (H - \Delta \ell)$$

as $r \longrightarrow \infty$, where H is the heat of reaction. Equation (2) may then be written as

$$\dot{m}_F \left[c_p (T - T_o) - (H - \Delta \ell) \right] = 4\pi r^2 \lambda_\ell (T/T_\ell) (dT/dr) \qquad (63)$$

for this region and is to be integrated between the limits r_c, T_c and ∞, T_o. After integrating and rearranging, the following expression is obtained for $\dot{m}_F$:

$$\dot{m}_F = \frac{4\pi \lambda_\ell r_c}{c_p T_\ell} \left\{ - \left[T_o + (H - \Delta \ell)/c_p \right] \ell n \left[1 - c_p (T_c - T_o/(H - \Delta \ell) \right] \right.$$

$$\left. - (T_c - T_o) \right\} . \qquad (64)$$

It is now possible to eliminate the parameter r_c between Equation (62) and (64) to obtain an expression for the mass burning rate in terms of known parameters.

$$\dot{m}_F = \frac{4\pi \lambda_\ell r_\ell}{T_\ell c_p} \left\{ \left[T_\ell - (\Delta \ell / c_p) \right] \ell n \left[1 + c_p (T_c - T_\ell)/\Delta \ell \right] + (T_o - T_\ell) \right.$$

$$\left. - \left[T_o + (H - \Delta \ell)/c_p \right] \ell n \left[1 - c_p (T_c - T_o)/(H - \Delta \ell) \right] \right\} . \qquad (65)$$

It should be noted that this simplified theory also predicts that the mass burning rate is proportional to the droplet radius.

By eliminating $\dot{m}_F$ from Equations (62) and (64), the following expression is obtained for r_c/r_ℓ

$$r_c/r_\ell = 1 - \frac{\left[T_\ell - (\Delta\ell/c_p)\right] \ln\left[1 + c_p(T_c - T_\ell)/\Delta\ell\right] + (T_c - T_\ell)}{\left[T_o + (H - \Delta\ell)/c_p\right] \ln\left[1 - c_p(T_c - T_o)/(H - \Delta\ell)\right] + (T_c - T_o)} . \tag{66}$$

It is seen that the value of r_c/r_ℓ is a constant during the burning of the drop according to this calculation. The value of T_c, which has been taken to be the adiabatic flame temperature, is calculated by conventional means, and will include the effects of dissociation.

The results of calculations made using this theory are somewhat different than those obtained through use of the diffusion theory. The flame temperatures are lower in the present case for two reasons, first, through the effects of dissociation, which tend to lower the temperature, and secondly, because the pre-heating of the fuel and oxidizer before they react at the flame zone is not taken into account. It is not possible to include the effects of pre-heat in the present analysis because the degree of pre-heat depends on the flame temperature, and vice versa; hence the problem would not be determinate. This difficulty is avoided in the diffusion theory through use of the mass transfer conditions. In that theory, the flame size depends on the rates of mass transfer, while the flame temperature depends on the rates of heat transfer. The flame

sizes as calculated from the present simplified thermal theory are considerably larger than those calculated by means of the diffusion theory. A comparison between the burning rates as calculated by the present thermal theory, the diffusion theory, and experiment will be carried out in Part V for droplets burning in atmospheres of differing oxygen content.

IV. EXPERIMENTS ON THE BURNING OF SINGLE FUEL DROPS

The original experiments of Godsave[7] yielded data on the burning rates of droplets of various hydrocarbon fuels suspended in air at room temperature and atmospheric pressure. It was found that the burning rates for the sixteen fuels tested did not vary widely. The burning rates, as represented by the evaporation constant, K'*, varied from 0.0077 cm^2/sec to 0.0099 cm^2/sec. Pure aliphatic and aromatic hydrocarbons, as well as two mixtures of hydrocarbons were used in these tests.

In order to provide further information on the burning of drops of pure hydrocarbon fuels under various atmospheric conditions, and to provide more stringent tests of the accuracy of the theories presented in Sections II and III, additional experiments have been performed in the course of this investigation. Specifically, the effect of variations of oxygen content, temperature, and pressure in the surrounding atmosphere, and the effect of forced convection on the burning rates of suspended fuel droplets have been investigated. The results of these tests are reported in the following paragraphs.

A. The General Combustion Apparatus

In order to provide means for experiments on burning of fuel drops under various conditions of temperature and pressure, a large combustion chamber has been constructed in the Mechanical Engineering Laboratory at the California Institute of Technology. The chamber is

---

* Godsave denotes the evaporation constant by the symbol λ.

made of stainless steel and consists of a thick-walled vertical tube, approximately 42 inches long and 7 inches in inside diameter. A group of twelve Chromalux 700 watt electrical heating elements are mounted in the walls of the tube, and approximately three inches of thermal insulation covers the outside tube wall to decrease heat loss. A thermostatic control operating a magnetic power relay permits the temperature of the gas within the tube to be varied from room temperature up to 1000^{o}F.

Ten quartz windows, 3/4 inch thick and 2 - 1/2 inches in diameter, are mounted in the walls of the tank to provide for visual or photographic observation. The windows are arranged in two vertical rows of five each, diametrically opposed. A sliding safety window covers each observation window, and may be retracted when photographs are to be taken.

Five thermocouple wells, each at the level of one of the window groups, permit the accurate determination of the internal gas temperature by use of iron-constantan thermocouples.

Heavy flanges are welded to the top and bottom of the tube, and are provided with studs and 'O'-ring grooves so that the top and bottom of the tank may be easily removed. Various items of equipment such as fuel injectors or ignition equipment may then be mounted in the tank head, and can be easily removed for adjustment. The tank is further provided with pipe leads to allow for pressurization or addition of various gases.

A heavy camera stand is mounted adjacent to the tank to provide

an adjustable, vibrationless support for motion picture equipment. The particular motion picture, pressurization, and injection apparatus used in the various portions of this investigation are described in the subsequent paragraphs.

B. The Effect of Varying Oxidizer Concentration

(1) Apparatus

The first set of experiments in this investigation was performed to study the change of droplet burning rates as the oxygen concentration was varied in the oxygen-nitrogen mixture surrounding a suspended droplet[23]. The experimental technique used in these experiments was similar to the method used by Godsave[7]. A motion picture camera was used to photograph a burning droplet of fuel suspended on a fine quartz filament. The filament and its support were mounted within the combustion tank described in the previous paragraph. A photograph of the tank, with its auxiliary apparatus, is shown in Figure 5. Compressed gas cylinders were used to provide the desired gas composition.

A fuel injection system was built into the head of the combustion tank. This system was provided with a fuel reservoir and means for pressurizing the reservoir. The fuel system was connected through a ball check valve to a hollow needle which extended approximately eight inches down into the tank.

A fine silica filament was cemented to the hollow needle, and was of such a length that its tip extended vertically down so as to be in the line of sight of the top windows of the tank. It was necessary to thicken the end of the filament in order to retain the liquid drop. The

diameter of the thickened end was approximately 0.3 mm.

The drops were suspended on the filament by pressurizing the reservoir, thereby forcing fuel through the hollow needle and onto the silica filament. The suspended drops were found to be between 1.5 and 1.8 mm in diameter. As can be seen from Figure 6, the suspended drops were reasonably spherical during the major part of their life.

The suspended drops were ignited by means of an electric spark. A standard automotive ignition circuit was utilized, with a manually operated on-off switch taking the place of the distributor breaker points. The high tension lead was brought into the tank through an appropriately modified spark plug screwed into the head of the tank. Steel rod approximately 1/16 inch in diameter was used for the spark gap electrodes. The spark gap was approximately 2 cm in length, and was adjusted so that the spark passed directly across the filament tip. This method of ignition was found to be satisfactory for oxygen concentrations greater than about 20 percent by weight in oxygen-nitrogen mixtures. At $Y_{O,o} = 0.15$ it was impossible to ignite a drop for the four fuels tested.

An electrically driven Bell and Howell "Eyemo" 35 mm motion picture camera was used to photograph the burning drops. The drops were photographed in silhouette by providing strong back lighting. A long focal length lens (6 in., f: 4.5 Cooke Teleking Anastigmat) mounted to the camera with a ten inch extention tube provided a magnification of about two diameters on the film.

The drops were photographed at a camera speed setting of

twenty-four frames per second. The actual camera speed at this setting was checked by photographing a calibrated stop watch, and was found to be 24.6 frames per second.

A 3/32 inch diameter ball bearing was photographed at the beginning and end of each 100 foot rool of film used. This calibration was carried out under the same camera focusing conditions as for the burning drops, thereby providing an accurate reference length on the film for determining the actual size of the droplets.

The size of the burning drops was determined by using a technique very similar to that described by Godsave[7]. The film was measured with the aid of a 35 mm microfilm reader (to produce further magnification) and a steel scale graduated to 1/100th of an inch. Two measurements were made on each frame, namely, the two perpendicular diameters inclined at 45^{o} to the major and minor axis in the plane of observation. The mean of these two measurements was recorded as the "effective diameter" of the drop. If the major and minor axes do not differ greatly, as was the case in these tests, then it is easily shown that the volume of a sphere with the measured effective diameter is not greatly different from that of the prolate spheroid which actually corresponds to the shape of the drop.

In most cases, measurements of each drop were taken over a range of size extending from ignition down to approximately one-half of the original drop diameter. For burning in air, every fifth frame of the film on each drop was measured. As the burning rate increased with increase in oxygen concentration, every two to four frames of the

film for any given drop were measured.

In order to vary the weight fraction of the oxygen ($Y_{O,o}$) in the atmosphere inside the combustion tank, a cylinder of compressed oxygen was connected through a regulator valve to the tank. Then, for example, for $Y_{O,o} = 0.50$, the combustion tank was pressurized to a gage pressure of 7.1 psi. The tank was kept at the required pressure for an extended time in order to allow complete mixing of the oxygen with the original air in the tank. The pressure in the tank was slowly decreased to the operating pressure, a drop of fuel suspended on the filament, the camera started, and the drop ignited. After each run the combustion tank was flushed with air before repeating the above process for another run. All combustion experiments were carried out at atmospheric pressure. It should be noted that for $Y_{O,o} = 0.15$ the combustion tank was pressurized with nitrogen to a gage pressure of 8.35 psi before bleeding to atmospheric pressure. However, ignition at this reduced oxygen concentration was impossible and no experimental data were obtained.

(2) Experimental Results

A systematic study was made to determine the evaporation constant, K', for different oxygen concentrations and for the following fuels: n-heptane, absolute ethyl alcohol, benzene, and toluene. The experimental results gave directly the droplet diameter, d, as a function of the time, t. The plots of d^2 against t were found to be linear. A typical experimental plot is shown in Figure 7. Thus the functional relation between drop diameter, d, and time, t,

$d^2 = d_0^2 - K't$, has been verified again. Here d_0 is the diameter at time $t = 0$ (corresponding to the beginning of steady burning) and K' is the evaporation constant. The value of K' is determined directly from the slope of plots of d^2 vs. t and has the dimensions $cm.^2\ sec.^{-1}$.

The experimentally determined values of K' for the four fuels tested at different oxygen weight fractions are listed in Table II. The

TABLE II. EXPERIMENTAL VALUES OF K' ($CM^2\ SEC^{-1}$) FOR SEVERAL FUELS AND WEIGHT FRACTIONS OF OXYGEN.

	Weight Fraction of Oxygen				
Fuel	$Y_{O,o}=0.23$	$Y_{O,o}=0.37$	$Y_{O,o}=0.50$	$Y_{O,o}=0.70$	$Y_{O,o}=0.90$
N-Heptane	8.35×10^{-3}	13.80×10^{-3}	15.01×10^{-3}	18.56×10^{-3}	22.34×10^{-3}
Ethyl Alcohol	8.58×10^{-3}	11.11×10^{-3}	15.04×10^{-3}	18.41×10^{-3}	20.36×10^{-3}
Benzene	9.85×10^{-3}	RESIDUE FORMATION			
Toluene	7.70×10^{-3}	RESIDUE FORMATION			

results of five separate experiments were examined for each fuel at each value of $Y_{O,o}$. The tabulated values of the evaporation constant are the mean values for each set of five runs. The reproducibility in each set of runs was good; the maximum spread of experimental data was found to be less than $\pm$ 1%.

With the lighting used for photography during the experiments, it was impossible to obtain pictures of the flames suitable for measurement of flame surface diameter. For n-heptane and ethyl alcohol the luminous flame surface was not sufficiently well-defined to permit

conclusions regarding flame shape and flame size. For benzene and toluene burning in air, the luminous region could be seen but was not sufficiently clear to yield accurate measurements.

(3) Residue Formation

For oxygen weight fractions exceeding 23 percent, formation of residue was observed during the burning of benzene and toluene. Photographs of droplets of benzene burning in atmospheres of various oxygen weight fractions are shown in Figure 8. The residue remaining on the filament at the conclusion of combustion was of a dry, brittle consistency. No chemical analysis of the residue was made. The formation of carbon in heterogeneous combustion of aromatic hydrocarbon fuels has been observed by other investigators and merits additional quantitative study.

Because of residue formation during the burning of benzene and toluene, it was impossible to determine accurately the burning rates of these fuels. The shroud-like formation of residue caused considerable distortion of the drop, and often completely surrounded and obscured the drop of fuel.

Carbon formation during the heterogeneous combustion of aromatic fuels, but not during the burning of aliphatic compounds, re-emphasizes the importance of chemical reaction rates, which have been neglected in the discussion of the diffusion model for droplet burning. According to one of the modern theories for carbon formation during burning[24], acetylene production is an essential intermediate step. One might therefore argue that the greater tendency of aromatic fuels

to form carbonaceous residues is related to the known ease with which these compounds form acetylene. This qualitative suggestion does not offer a satisfactory explanation for the dependence of residue formation on oxygen concentration.

A possible explanation for this variation in residue formation is the following: as the oxygen concentration is increased, the temperature of the flame zone becomes higher, and tends to increase pyrolysis of the aromatic fuel. The lighter compounds and radicals (e.g., acetylene) thereby produced then polymerize in the cooler tip of the flame. This process continues until the burning droplet is extinguished because of the growth of the residue.

If the oxygen concentration is further increased, the residue formed is itself capable of being burned although at a lower rate than the liquid fuel. The consumption of the residue may be noted in the two bottom rows of photographs in Figure 8.

In order to describe quantitatively the formation of carbon in heterogeneous combustion, it is clearly necessary to allow for the interdependence of chemical reaction rates, mass transport by concentration and thermal diffusion, and energy transport by thermal conduction.

C. The Effect of Ambient Pressure on Burning Rate

The influence of increased atmospheric pressure on the burning rates of droplets of various hydrocarbons burning in air has been investigated by Hall and Diederichsen [25]. In their experiments, suspended droplets of furfuryl alcohol, tetratin, decane, and amyl acetate were burned in air at pressures ranging from one to twenty

atmospheres. The measurements showed that the mass burning rate of a droplet is proportional to the drop diameter.

The data for furfural alcohol and tetralin indicate that the burning rate, or K', is proportional to the pressure raised to the 0.2 power; data for decane and amyl acetate indicate that burning rate is proportional to pressure raised to the power 0.3. Hall and Diederichsen conclude that the mass burning rate is roughly proportional to the one-fourth power of the pressure for hydrocarbons burning in air.

They also studied the size and shape of the flame front surrounding the liquid droplets. In contrast to the data of Godsave[7], which indicated that the ratio of flame to drop size is a constant, Hall and Diederichsen report that the distance between the flame front and the drop surface appeared to be constant during burning.

Primarily in connection with the residue formation behavior exhibited by some aromatic fuels as reported in Part B of this section, it was thought desirable to study the influence of air pressure on the burning behavior of drops of benzene, a typical aromatic. The apparatus and experimental technique used was identical to that used for the measurements discussed in Part B. Owing to the limitations of the spark ignition method, data were obtained only up to a pressure of five atmospheres.

The results of these experiments are shown in Figure 9, where $\log K'$ is plotted as a function of $\log p$. Reference to Figure 9 shows that the burning rate of benzene drops in air is roughly proportional to the 0.4 power of the pressure. No residue formation in excess of that

found for burning at atmospheric pressure was noted at the higher pressures.

D. Effect of Increased Ambient Temperature on Drop Burning Rates

Another parameter of interest in its effect on droplet burning rate is the temperature of the surrounding oxidizing atmosphere. In his investigations of the rate of evaporation of droplets suspended in a hot gas, Kobayashi[26] found that at ambient temperatures of about 700°C hydrocarbon drops underwent auto-ignition. Therefore, in a further investigation[27], Kobayashi measured the mass burning rates of droplets burning in air at temperatures up to 900°C. Again it was found that mass burning rate is proportional to drop diameter.

The experimental technique used by Kobayashi utilized the suspension of the droplet on a quartz fiber outside the combustion chamber. The heated chamber was mounted on rails, and was then moved over the drop and its suspending fiber. Motion pictures were taken of the burning droplet through windows in the chamber walls. Mass burning rates could then be calculated from the decrease in size of the drop image with time. Kobayashi's data show considerable scatter. His results for two fuels, n-heptane and benzene, are listed in Table III.

In order to provide data for temperatures intermediate between room temperature and the high temperatures reported in Kobayashi's work, measurements of burning rates have been made in the course of the present investigation. Details of experimental technique and results are reported in the following paragraphs.

TABLE III. EXPERIMENTAL VALUES OF K' (CM^2-SEC^{-1}) FOR TWO FUELS BURNING IN AIR AT ELEVATED TEMPERATURE (KOBAYASHI[27]).

N-Heptane		Benzene	
T_o(°C)	K' (cm^2-sec^{-1})	T_o(°C)	K' (cm^2-sec^{-1})
700	0.0121	710	0.0100
	0.0110		0.0122
800	0.0124	730	0.0105
			0.0108
			0.0090
		735	0.0101
		750	0.0087
			0.0091
			0.0096
			0.0111
		800	0.0116
			0.0137

(1) Apparatus

For the purposes of these experiments a new injection apparatus was built into the head of the combustion tank. The spark ignition device was essentially the same as that used for the experiments described in Part B. For these tests, the injector consisted of two

concentric tubes. Air was passed through the annulus so formed to cool the injector. The inner tube extended down into the tank about six inches, and the fine quartz fiber used for suspending the liquid drop was affixed to its tip. To suspend the droplets on the quartz fiber, a hypodermic syringe with a specially constructed needle was used. This long needle was inserted through the inner tube of the injector until its tip was near the tip of the silica filament. A droplet could then be forced from the hypodermic needle and would then flow to the fiber tip. After withdrawing the hypodermic needle, the drop was ignited with the sparking device.

An Arriflex 35 mm electrically driven motion picture camera was used for these measurements. To obtain large images of the droplets, a 125 mm Astro Pan-Tachar telephoto lens was mounted on the camera with a four inch extention tube. Strong back lighting was used to give clear images. Camera speed was approximately 25 frames per second, and a timing device, arranged to periodically interrupt the light reaching the lens, provided accurate timing marks on the film. The method of obtaining the effective droplet diameter from the film images was the same as described in Part B of this section.

(2) Experimental Results

Data were obtained for the burning rates of benzene and n-heptane at temperatures of about 140°C (300°F). At somewhat higher temperatures it was found that the droplets would not adhere to the quartz fiber and fell off as soon as they were formed. At still higher temperatures, the liquid fuel was vaporized while flowing through the hypodermic needle, hence no drops could be formed.

For these reasons, only a limited number of data could be obtained using this injection device. Also, owing to the discrepancy between these data and the results of other investigations (see Figures 14 and 15), even the limited data obtained are subject to question. A possible explanation for the discrepancy may be that an appreciable amount of the heat necessary for evaporation may have been supplied from the hot quartz fiber. An attempt was made to reduce this error by flowing a stream of the liquid fuel over the quartz fiber before suspending the droplet whose burning rate was studied.

A summary of the data obtained in these tests is presented in Table IV. In contrast to the highly reproducible data obtained in the

TABLE IV. EXPERIMENTAL VALUES OF K' (CM^2-SEC^{-1}) FOR FUELS BURNING IN AIR AT ELEVATED TEMPERATURE.

N-Heptane		Benzene	
T_o(°C)	K'(cm^2-sec^{-1})	T_o(°C)	K' (cm^2-sec^{-1})
135	0.0115	120	0.0123
	0.0116		0.0144
	0.0115		0.0120
	0.0116		0.0129
	0.0111		0.0130
	0.0110		0.0130

experiments reported in Part B, considerable scatter was found in the present case.

E. Effect of Forced Convection on Drop Burning Rates

All of the experiments described thus far have been performed with droplets burning in a quiescent atmosphere subject only to the effects of free convection. It was therefore thought to be of interest to investigate the influence of forced convection on a burning droplet. In order to obtain an accurate quantitative description of droplet burning rates as a function of the physico-chemical parameters and the flow conditions, an extensive experimental program would be necessary. The time and expense involved in such an elaborate investigation precluded its inclusion in the present program.

However, a more modest series of experiments was performed in order to answer two important questions concerning the effects of forced convection. These questions are: 1) What is the order of magnitude of change of burning rate caused by forced convection? 2) At what gas velocity is the flame surrounding the droplet extinguished, i.e., "blown off"? A description of these experiments and of the results will now be presented.

(1) Apparatus

The large combustion tank was not used for experiments on the influence of forced convection on burning rate. Instead, the droplets were suspended on a quartz fiber in a small duct through which air could be blown. The duct was constructed of lucite tubing, two inches in inside diameter and approximately one foot long. The duct was held vertically with the air flowing upward. The air was introduced at the bottom of the duct, and flowed through two baffle plates and three fine

screens before passing over the drop. The purpose of the baffle plates and screens was to insure a fairly flat velocity profile across the diameter of the duct.

The air flow was metered by a Fischer and Porter Laboratory Flowrator. The linear air velocity in the duct was obtained by dividing the volume flow rate by the cross-sectional area of the duct. The laboratory air supply was used for these tests.

A quartz fiber was inserted downward into the exit of the duct. The droplets were suspended on the tip of the fiber by means of a hypodermic syringe. Again, ignition was accomplished by means of an electric spark. The electrodes were mounted in the duct wall, with a gap of approximately two centimeters between their tips. The fiber was mounted midway in this gap. The Arriflex motion picture camera described in Part D of this section was used to study the burning of the droplets.

(2) Experimental Results

Droplet diameter vs. time histories were obtained for n-heptane, ethyl alcohol, and benzene burning in air streams of velocities up to 40 cm/sec. In order to obtain the functional dependence of droplet burning rate on the flow parameters (e.g., Reynolds Number) from a set of diameter vs. time plots, extremely accurate data are necessary to define the second derivative of the droplet diameter vs. time curve. The present experimental technique does not yield sufficiently accurate diameter histories to permit this type of analysis. Instead, the method of analysis used for the still atmosphere experiments was employed,

where the square of the droplet diameter was plotted as a function of time. Data for a still atmosphere (except for free convection currents) yielded straight line plots when presented in this way; the present data, on the other hand, showed irregular, but relatively small deviations. A typical plot is shown in Figure 10. Although it was not proved that the mass rate of fuel consumption is accurately proportional to the drop diameter under conditions of forced convection, it was possible to fit a straight line to the plots of d^2 vs. t and, therefore, to obtain an effective value for K', the evaporation constant. The values for the effective evaporation constants evaluated in this way are presented in Table V. Each value reported is the average of values found for three separate runs. The individual values varied from the average value by no more than $\pm$ 5 $^{o}/o$.

It is seen that the droplet burning rates, as represented by the effective evaporation constant, are increased up to a maximum of thirty-six percent at the highest gas velocities used in these tests. At gas velocities higher than the largest values shown in Table V, the burning droplets were extinguished. It may be seen that these velocities are quite low, in no case exceeding 40 cm/sec.

Spalding[28] has investigated the flame blow-off phenomenon for porous spheres covered by a liquid film of fuel. The spheres were immersed in an air stream. He reports that as the air velocity was increased, the flame that had heretofore surrounded the sphere was altered so as to burn only behind the sphere. The flame remained attached to the surface, however, and resembled the flame front

TABLE V. EFFECTIVE VALUES OF THE EVAPORATION CONSTANT, K', FOR N-HEPTANE, ETHYL ALCOHOL, AND BENZENE DROPLETS BURNING IN AN AIR STREAM.

Fuel	Air Velocity (cm/sec)	Effective K' ($cm^2 - sec^{-1}$)	Effective K'/Still Air K'
N-Heptane	0	8.4×10^{-3}	1.00
	11.8	10.2	1.22
	26.9	11.0	1.32
	34.5	11.4	1.36
Ethyl Alcohol	0	8.6×10^{-3}	1.00
	11.8	9.0	1.05
	26.9	9.6	1.12
	39.4	10.7	1.25
Benzene	0	9.9×10^{-3}	1.00
	11.8	10.4	1.06
	26.9	11.5	1.17
	34.5	13.1	1.33

observed for the case of cylindrical flame holders in a stream of premixed fuel and air. At still higher velocities, Spalding reports that the flame burned in the wake of the sphere, and was not attached to the surface. This progression of blow-off phenomena was not observed in the present investigation of droplet burning.

It is quite likely that the supporting quartz fiber may exert considerable influence on the flame blow-off behavior. For this reason it would be advisable to study blow-off by the use of droplets falling freely through the oxidizing gas.

V. COMPARISON OF THEORY AND EXPERIMENT

In this section, the results of the experiments discussed in the previous section will be compared to the predictions of the droplet combustion theories presented in Sections II and III. It has already been pointed out that the thermal theory, because of the simplified reaction rate law used, predicts no change in droplet burning rate as the oxidizer concentration in the surrounding atmosphere is varied. On the other hand, the simplified thermal theory presented in Part C of Section III, as well as the diffusion theory of Section II, predict appreciable dependence of drop burning rate on oxidizer concentration. The experimental data of Part B, Section IV, show a definite dependence of burning rate, or evaporation constant, on this parameter. Therefore, the detailed comparison of experimental and theoretical results will be made only for the simplified thermal theory and the diffusion theory.

A. Comparison of the Results of the Simplified Thermal Theory and Experiment

The experimental values of K', the evaporation constant, for droplets of n-heptane and ethyl alcohol burning in various oxygen-nitrogen mixtures were presented in Table II on page 51. In the following table, values of K' as computed by the simplified thermal theory are presented for n-heptane burning in air and pure oxygen. The adiabatic flame temperature was obtained by use of prepared charts[29]. These theoretically calculated values of K' are plotted as a function of oxygen weight fraction in Figure 11, together with the experimental results.

TABLE VI. CALCULATED VALUES OF T_c, r_c/r_ℓ , AND K' FOR THE BURNING OF DROPS OF N-HEPTANE ACCORDING TO THE SIMPLIFIED THERMAL THEORY.

$Y_{O,o}$	T_c (^oK)	r_c/r_ℓ	K' (cm^2-sec^{-1})
0.23	2290	23.4	0.0107
1.00	3140	17.3	0.0151

Reference to Figure 11 reveals that the simplified thermal theory does not provide an adequate correlation for the experimental data. It will be seen in the following paragraphs, however, that the diffusion theory is quite accurate in predicting the variation in burning rate with increasing oxygen concentration. On the basis of this comparison, the simplified thermal theory will be rejected as inadequate, and further detailed comparisons between theory and experiment will be made only for the case of the diffusion theory. The theoretical shortcomings of the thermal theories have already been discussed in Section III.

B. Comparison of the Results of the Diffusion Theory and Experiment

Calculated values of K' for several fuels burning in air at atmospheric pressure and room temperature were listed in Table I, page 27. In Table II, page 51, the corresponding experimental values of K' were presented. In the following Table VII these values

are compared, and satisfactory agreement is noted.

TABLE VII. COMPARISON OF CALCULATED AND OBSERVED VALUES FOR THE EVAPORATION CONSTANT, K', FOR SEVERAL HYDROCARBONS BURNING IN AIR.

Compound	Observed Value of K' (cm^2-sec^{-1})	Calculated Value of K' (cm^2-sec^{-1})
Benzene	0.0098	0.0102
Ethyl Alcohol	0.0086	0.0079
N-Heptane	0.0084	0.0086
Toluene	0.0077	0.0087

(1) Comparison of Observed and Calculated Values of r_c/r_ℓ

It is of interest to compare the values of flames size as observed by Godsave and the calculated values according to the diffusion theory. The theoretical analysis is based on the assumption that a spherical reaction surface surrounds the burning droplet. On the other hand, photographs of burning droplets, e.g., Figure 1, show that the flame zone is much elongated, owing to the effects of free convection. Godsave[7] measured the radius of the roughly hemispherical bottom portion of the flame zone, and stated that the ratio of this radius to the droplet radius is a constant, characteristic for the fuel, when burning in air. The values of r_c/r_ℓ calculated from Equation (27) are contrasted in Table VIII with the values of r_c/r_ℓ deduced by

TABLE VIII. COMPARISON OF CALCULATED AND OBSERVED COMBUSTION RADII .

Fuel	r_c/r_ℓ Observed Values	r_c/r_ℓ Calculated Values
Benzene	3.0	9.6
n-Heptane	3.0	8.5
Toluene	2.6	9.5

Godsave from his photographs of burning fuel drops. Reference to Table VIII shows that the calculated values are appreciably larger than the observed data. There are several obvious reasons for the observed discrepancies. Thus reference to Figure 1 shows that the "still" droplet was subjected to strong free convection currents during burning; the value of r_c/r_ℓ for a spherical surface with area equivalent to the area of the observed luminous zone is roughly double that of Godsave's tabulated values.

Furthermore, it is not evident that the reaction surface in the idealized model should, in fact, be identified with the region of maximum luminosity. The surface for maximum temperature gradients, as determined from schlieren photographs[7], corresponds to larger "observed" values of r_c/r_ℓ than are listed in Table VIII.

The discrepancies between calculated and measured values of r_c/r_ℓ emphasize also the need for refinement in the theoretical description of the burning process. Thus it is apparent that the introduction of a spherical reaction shell of finite thickness will lead to lower

values of T_c and also to lower effective values of r_c/r_ℓ ; as indicated in the footnote on page 22 , a similar effect is produced also if proper allowance is made for dissociation by assuming that chemical equilibrium is established at every point. Presumably the changes in T_c and r_c/r_ℓ will largely compensate for each other in the calculation of $\dot{m}_F$, or K', thereby accounting for the satisfactory agreement between calculated and observed values of $\dot{m}_F$.

It seems appropriate to note again that some experimental evidence exists which is not in accord with the idea that r_c/r_ℓ is a constant. It has been pointed out that Hall and Diederichsen[25] have stated that their studies of the burning of single drops suggest that the distance between the flame front and the drop surface remains constant during burning.

(2) Effect of Increasing Oxygen Concentration

In Table IX, the values of K', T_c, and r_c/r_ℓ as computed by the diffusion theory are presented for n-heptane and ethyl alcohol burning in various oxygen-nitrogen mixtures. As would be expected, the flame temperatures rise with increasing oxygen concentration, while the ratio of flame radius to drop radius decreases. The extremely high computed flame temperatures result directly from the fact that the effects of dissociation have been neglected in the theoretical analysis. In spite of these unrealistic calculated flame temperatures, the calculated values of the evaporation constant, K', are found to be in satisfactory agreement with the experimentally determined values. A comparison of experimental and theoretical values of K' is carried out

TABLE IX. CALCULATED VALUES FOR DROPS OF N-HEPTANE AND ETHYL ALCOHOL BURNING IN VARIOUS OXYGEN-NITROGEN MIXTURES ACCORDING TO THE DIFFUSION THEORY.

	$Y_{O,o}=0.10$	$Y_{O,o}=0.23$	$Y_{O,o}=0.37$	$Y_{O,o}=0.50$	$Y_{O,o}=0.70$	$Y_{O,o}=0.90$
N-Heptane						
T_c (^oK)	1694	3225	4555	5575	6810	7755
r_c/r_ℓ	19.02	8.58	4.51	3.88	2.91	2.39
K' (cm^2/sec)	4.85×10^{-3}	8.58×10^{-3}	12.35×10^{-3}	14.58×10^{-3}	18.52×10^{-3}	22.50×10^{-3}
Ethyl Alcohol						
T_c (^oK)	1687	3110	4280	5110	6080	6780
r_c/r_ℓ	8.70	5.30	3.62	2.82	2.30	1.99
K' (cm^2/sec)	3.88×10^{-3}	7.91×10^{-3}	11.64×10^{-3}	14.95×10^{-3}	19.47×10^{-3}	24.00×10^{-3}

in Table X. A graphical comparison is made in Figures 12 and 13, where experimental and theoretical values of K' for n-heptane and ethyl alcohol are plotted as a function of $Y_{O,o}$.

The satisfactory agreement between the calculated and the experimental values of K' suggests that the physical model upon which the theoretical analysis is based represents a useful first approximation for predicting the burning rates of single drops of the fuels considered. The success of the theory must be ascribed to nearly complete compensation between the obvious deficiencies of the analysis.

(3) The Influence of Pressure on Droplet Burning Rate

According to the diffusion theory of droplet combustion, little change in burning rate is to be expected as the pressure in the surrounding atmosphere is increased. The only influence of pressure on the final expression for the evaporation constant is due to the change in normal boiling point, density, and latent heat of vaporization of the liquid fuel. These effects are small and do not account for the comparatively larger changes observed experimentally by Hall and Diederichsen[24] and in the present investigation.

Several explanations might be offered for this discrepancy. Chemical reaction rates are sensitive functions of the pressure (for a complicated process, an overall dependence for the reaction rate on the square of the pressure is not unreasonable) and, therefore, a very weak dependence of burning rate on reaction rates could account for the observed variation. Furthermore, the effects of radiant heat transfer to the liquid fuel, which were neglected in the diffusion theory, increase rapidly with pressure and could account for a weak dependence of burning

TABLE X. COMPARISON BETWEEN THEORETICAL AND EXPERIMENTAL VALUES OF K' FOR DIFFERENT VALUES OF $Y_{O,o}$.

Fuel	Weight Fractions of Oxygen				
	$Y_{O,o}$=0.23	$Y_{O,o}$=0.37	$Y_{O,o}$=0.50	$Y_{O,o}$=0.70	$Y_{O,o}$=0.90
N-Heptane					
Theory	8.58×10^{-3}	12.35×10^{-3}	14.58×10^{-3}	18.52×10^{-3}	22.50×10^{-3}
Experiment	8.35×10^{-3}	13.80×10^{-3}	15.01×10^{-3}	18.56×10^{-3}	22.34×10^{-3}
Ethyl Alcohol					
Theory	7.91×10^{-3}	11.64×10^{-3}	14.95×10^{-3}	19.47×10^{-3}	24.00×10^{-3}
Experiment	8.58×10^{-3}	11.11×10^{-3}	15.04×10^{-3}	18.41×10^{-3}	20.36×10^{-3}
Benzene					
Theory	10.02×10^{-3}				
Experiment	9.85×10^{-3}				
Toluene					
Theory	8.72×10^{-3}				
Experiment	7.70×10^{-3}				

rate on ambient pressure.

It has been proposed that the inevitable convection currents may lead to a slight variation in burning rate with pressure. It has been pointed out by Lorell and Wise[18] that the conventional heat transfer correlations indicate that the heat transfer coefficient for a sphere under conditions of free convection is proportional to the one-fourth power of the pressure. They suggest, by analogy, that it is the influence of pressure on the free convection currents surrounding the burning droplet that accounts for the observed variation in burning rate. However, the experiments on forced convection indicate that only a small increase in burning rate is to be expected as the flow velocity resulting from free convection is increased, as the free convection velocity is a few centimeters per second. Therefore this explanation for the increase in burning rate should be rejected.

(4) The Influence of Increased Ambient Temperature on Burning Rate

The diffusion theory predicts an increase in burning rate, and hence of K', with increasing ambient temperature. A summary of calculated results for n-heptane and benzene burning in air at elevated temperatures is presented in Table XI. As has been noted, considerable scatter exists in the data of Kobayashi[27] for burning measurements made at high temperatures. Some doubt exists also as to the validity of the data taken at lower temperatures in the course of the present investigation. However, both sets of data are presented in Figures 14 and 15, together with the predictions of the diffusion theory. Fair agreement is noted, in contrast to the excellent agreement obtained

for the variation of K' with gas composition.

TABLE XI. CALCULATED VALUES FOR THE BURNING OF DROPS OF N-HEPTANE AND BENZENE AT ELEVATED TEMPERATURES ACCORDING TO THE DIFFUSION THEORY.

n-Heptane			
$T_o(^oK)$	$T_c(^oK)$	r_c/r_ℓ	$K'(cm^2\text{-}sec^{-1})$
300	3230	8.6	0.0086
410	3300	8.3	0.0090
800	3600	7.7	0.0096
1025	3780	7.3	0.0101
Benzene			
$T_o(^oK)$	$T_c(^oK)$	r_c/r_ℓ	$K'(cm^2\text{-}sec^{-1})$
300	3450	9.6	0.0100
425	3510	9.5	0.0101
700	3730	8.5	0.0104
1025	3990	8.4	0.0112

Since the diffusion theory makes no allowance for the mass or heat transport by natural or forced convection, it is not possible to compare the observed dependence of K' on flow velocity with theoretical predictions.

C. Conclusions

The comparisons between theory and experiment made in the preceding paragraphs suggest that the physical model upon which the diffusion theory is based represents a useful first approximation for

the fuel-oxidizer systems considered. However, there are serious doubts that the basic physical assumptions involved in this model are applicable to certain chemical systems, where the rates of chemical reaction are slow, or extensive decomposition of the fuels may occur without the presence of oxidizer. For example, in a recent investigation[30], it was found that the diffusion theory satisfactorily predicted the burning behavior of nitromethane in air, but was inadequate to explain the observed burning rates of hydrazine in air. It is known that the activation energy for the decomposition of hydrazine is quite low, however, and considerable exothermic decomposition may take place before the hydrazine and its decomposition products are oxidized.

In spite of the apparent deficiencies in the state of knowledge concerning the burning behavior of isolated, single drops, it appears that the most important subject for future research in this field is the relation of single droplet burning to fuel spray combustion behavior. An attempt has been made recently by Graves[31] to correlate known droplet burning rates with observed turbojet combustor performance. The variation of experimentally observed burning rates of iso-octane droplets in various oxygen-nitrogen mixtures was used to try to predict the change in combustion efficiency of a turbojet combustion can as the initial conditions of the inlet gas were varied. The predicted increase in combustion efficiency as the inlet oxygen concentration is raised fell short of the increased combustion efficiency observed in actual combustion chamber tests. This result suggests that the relation of single droplet burning to spray combustion must be carefully investigated before the results of research on single droplets can be considered useful for the overall spray combustion problem.

REFERENCES

1. M. Gerstein, "Some Problems Pertinent to the Combustion of Sprays", presented before AGARD Combustion Panel, Scheveningen, Netherlands, (May 1954).

2. W. E. Ranz and W. R. Marshall, Jr., "Evaporation from Drops"; Part I, Chemical Engineering Progress, vol. 48, (1952), pp. 141-146; Part II, Chemical Engineering Progress, vol. 48 (1952), pp. 173-180.

3. R. D. Ingebo, "Vaporization Rates and Heat Transfer Coefficients for Pure Liquid Drops", Nat. Advis. Comm. for Aero. Technical Note TN 2368, (July 1951).

4. R. D. Ingebo, "Study of Pressure Effects on Vaporization Rate of Drops in Gas Streams", Nat. Advis. Comm. for Aero. Technical Note TN 2850, (January 1953).

5. R. D. Ingebo, "Vaporization Rates and Drag Coefficients for Iso-Octane Sprays in Turbulent Air Streams", Nat. Advis. Comm. for Aero. Technical Note TN 3265, (October 1954).

6. D. B. Spalding, "The Combustion of Liquid Fuel in a Gas Stream", Part I, Fuel, vol. XXIX, (January 1950), p. 2-7; Part II, Fuel, vol. XXIX, (February 1950), pp. 25-32.

7. G. A. E. Godsave, "Studies of the Combustion of Drops in a Fuel Spray - The Burning of Single Drops of Fuel", Fourth Symposium (International) on Combustion, Williams and Wilkins Company, Baltimore, (1953), pp. 819-830.

8. S. P. Burke and T. E. W. Schumann, "Diffusion Flames", Industrial and Engineering Chemistry, vol. 20, (1928), pp. 998-1004.

9. H. G. Wolfhard and W. G. Parker, "A Spectroscopic Investigation into the Structure of Diffusion Flames", Proc. Royal Society, A, vol. LXV, (1952), pp. 2-19.

10. H. C. Hottel and W. R. Hawthorne, "Diffusion in Laminar Flame Jets", Third Symposium (International) on Combustion, Williams and Wilkins Company, Baltimore, (1949), pp. 254-266.

11. S. Kumagai and H. Isoda, "Experimental Study on Evaporation and Combustion of Fuel Droplet", Science of Machine, vol. 4, (1952), pp. 337-342.

12. S. Kumagai and A. Kimura, "Combustion of Fuel Droplets", Science of Machine, vol. 3, (1951), pp. 431-434.

13. J. E. C. Topps, "An Experimental Study of the Evaporation and Combustion of Falling Drops", J. of the Institute of Petroleum, vol. 37, (1951), pp. 535-537.

14. S. S. Penner, "On Maximum Evaporation Rates of Liquid Droplets in Rocket Motors", J. of the American Rocket Society, vol. 23, (1953), pp. 85-88.

15. F. W. Hartwig, "Maximum Evaporation Rates for Non-Isothermal Droplets", J. of the American Rocket Society, vol. 23, (1953), pp. 242-243.

16. B. P. Mullins, "Studies on the Spontaneous Ignition of Fuels Injected in a Hot Air Stream"; Part I, Nat. Gas Turbine Establishment (Great Britain) Report No. R. 89, (1951); Part II, Nat. Gas Turbine Establishment (Great Britain) Report No. R. 90, (1951).

17. G. A. E. Godsave, "The Combustion of Drops in a Fuel Spray", Nat. Gas Turbine Establishment (Great Britain) Memorandum No. M. 95, (1950).

18. J. Lorell and H. Wise, "Steady-State Burning of Liquid Drops", Jet Propulsion Laboratory Progress Report No. 20-237, California Institute of Technology, Pasadena, California, (1954).

19. Y. H. Kuo, private communication, (May 1954).

20. N. N. Semenov, "Thermal Theory of Combustion and Explosion", Nat. Advis. Comm. for Aero. Technical Memorandum TM 1024, (August 1942); Progress of Physical Science (U.S.S.R.), vol. 23, (1940), No. 3.

21. M. Goldsmith and S. S. Penner, "On the Burning of Single Drops of Fuel in an Oxidizing Atmosphere", Technical Report No. 2, Office of Ordnance Research, California Institute of Technology, Pasadena, California, (October 1953); Jet Propulsion, vol. 24, (1954), pp. 245-251.

22. "Handbook of Chemistry and Physics", Chemical Rubber Publishing Company, Cleveland, 33rd Ed., (1951), p. 1579.

F. D. Rossini, et. al., "Selected Values of Properties of Hydrocarbons", circular of Nat. Bureau of Standards, C.461, U. S. Department of Commerce, (November 1947).

J. B. Maxwell, "Data Book on Hydrocarbons", Van Nostrand, New York (1950).

23. M. Goldsmith and C. K. Perkins, "Experiments on the Burning of Single Drops of Fuel in Oxygen-Inert Gas Mixtures", Technical Report No. 4, Office of Ordnance Research, California Institute of Technology, Pasadena, California, (May 1954).

24. G. Porter, "Carbon Formation in the Combustion Wave", Fourth Symposium (International) on Combustion, Williams and Wilkins Company, Baltimore, (1953), pp. 248-252.

25. A. R. Hall and J. Diederichsen, "An Experimental Study of the Burning of Single Drops of Fuel in Air at Pressures up to Twenty Atmospheres", Fourth Symposium (International) on Combustion, Williams and Wilkins Company, Baltimore, (1953), pp. 837-846.

26. K. Kobayashi, "A Study on the Evaporation Velocity of a Single Liquid Droplet", Technology Reports of the Tohoku University, Sendai, Japan, vol. XVIII, (1954), pp. 209-222.

27. K. Kobayashi, "An Experimental Study on the Combustion of a Single Fuel Droplet", Technology Reports of the Tohoku University, Sendai, Japan, vol. XVIII, (1954), pp. 223-234.

28. D. B. Spalding, "Experiments on the Burning and Extinction of Liquid Fuel Spheres", Fuel,vol. 32, (1953), pp. 169-185.

29. H. C. Hottel, G. C. Williams, and C. N. Satterfield, "Thermodynamic Charts for Combustion Processes - Part I", John Wiley and Sons, New York, (1949).

30. D. W. Kylie, "On the Burning of Monopropellant Drops", Technical Report No. 10, Office of Ordnance Research, California Institute of Technology, Pasadena, California, (May 1955).

31. C. C. Graves, "Burning Rates of Single Fuel Drops and Their Application to Turbojet Combustion Process", Nat. Advis. Comm. for Aero., Research Memorandum No. RM E53E22, (July 1953).

32. J. H. Burgoyne and L. Cohen, "The Effect of Drop Size on Flame Propagation in Liquid Aerosols", Proc. Royal Society, A, vol. 225, (1954), pp. 375-392.

33. B. Lewis and G. Von Elbe, "Combustion, Flames, and Explosions of Gases", Academic Press, New York, (1951), p. 340.

34. S. Chapman and T. G. Cowling, "The Mathematical Theory of Non-Uniform Gases", Cambridge University Press, (1939), Chapter 14.

APPENDIX A

Momentum Equation for Flow Field Surrounding the Burning Droplet

The momentum equation for a flowing fluid must be used to check the validity of the assumption that the pressure is essentially constant in the region surrounding a burning droplet. For the steady-state flow of a perfect fluid (the effect of viscosity will be ignored), the momentum equation may be written in the following vector form:

$$\rho \underline{u} \cdot \nabla \underline{u} = - \nabla p . \qquad \text{(A-1)}$$

In this notation ρ and p are the density and pressure, respectively, and $\underline{u}$ is the vector velocity.

In the present spherically symmetric problem, the velocity is directed outward from the droplet radially, and has the following magnitude,

$$u = \dot{m}_F / 4\pi r^2 \rho . \qquad \text{(A-2)}$$

Equation (A-1) may now be written

$$\left[\frac{\dot{m}_F}{4\pi r^2 \rho} \right] \times \frac{1}{r^2} \times \frac{d}{dr} \left[r^2 \left\{ \frac{\dot{m}_F}{4\pi r^2 \rho} \right\} \right] = - \frac{dp}{dr} , \qquad \text{(A-3)}$$

or

$$\left[\frac{\dot{m}_F}{4\pi} \right]^2 \times \frac{1}{r^4 \rho^2} \times \frac{d\rho}{dr} = \frac{dp}{dr} . \qquad \text{(A-3a)}$$

It is desired to evaluate the quantity dp/p; for $|dp/p| \ll 1$, the assumption of constant pressure in the flow field surrounding the droplet

is validated. This quantity may be approximated by

$$|dp/p| \simeq \left[\frac{\dot{m}_F}{4\pi}\right]^2 \frac{1}{pr^4\rho} \quad . \tag{A-4}$$

As the mass burning rate, $\dot{m}_F$, is proportional to the drop radius, which is a characteristic dimension of the system, Equation (A-4) may be rewritten as

$$|dp/p| \simeq \left[\frac{\dot{m}_F}{r_\ell}\right]^2 \times \frac{1}{16\pi^2 r_\ell^2 \rho p} \quad . \tag{A-4a}$$

Typical values of the quantities in Equation (A-4a) for a hydrocarbon burning in air at one atmosphere pressure are

$$(\dot{m}_F/r_\ell) = 10^{-2} \text{ (gm/cm-sec)}$$

$$\rho = 10^{-3} \text{ gm/cm}^3$$

$$p = 10^3 \text{ gm/cm-sec}^2 .$$

Hence

$$|dp/p| \simeq 0.6 \times 10^{-6}/r_\ell^2 .$$

As the droplet size decreases, the value of dp/p increases. The use of the drop radius as the characteristic dimension of the system results in a conservative estimate. For a droplet of 0.005 cm. (50 microns) diameter

$$|dp/p| \simeq 0.1 ,$$

hence the approximation of constant pressures is still reasonable for droplets of this size. It has been reported by Burgoyne and Cohen[32] that droplets smaller then this do not seem able to sustain combustion

individually. Therefore it may be concluded that the assumption of constant pressure flow field is valid for the case of a burning droplet.

APPENDIX B

Derivation of the Diffusion Equation

The general conservation equation for a non-reacting gaseous species k is given by[33]

$$\partial C_k/\partial t = -\nabla \cdot \left[C_k (\bar{v} + \bar{V}_k)\right] \tag{B-1}$$

where C_k is the molar concentration of species k, $\bar{v}$ is the mass-weighted average velocity of the gas mixture, and $\bar{V}_k$ is the diffusion velocity of species k. For the purposes of the present analysis, only binary (two componant) systems will be considered. For such a system the following expressions may be written[34],

$$Y_1 \bar{V}_1 + Y_2 \bar{V}_2 = 0 \tag{B-2}$$

and

$$\bar{V}_1 - \bar{V}_2 = - \frac{C_T^2}{C_1 C_2} D_{12} \left[\nabla \frac{C_1}{C_T} \right], \tag{B-3}$$

where Y_k is the weight fraction of species k, C_T is the total concentration (moles/unit volume), and D_{12} is the binary diffusion coefficient for the interdiffusion of species 1 and 2. Equation (B-3) accounts only for the occurrence of concentration diffusion; diffusion resulting from pressure or temperature gradients is ignored.

By definition,

$$C_k = \rho Y_k/M_k , \tag{B-4}$$

where ρ is the gas density and M_k is the molecular weight of species k. As the sum of the weight fractions must equal 1, we have

$$Y_1 + Y_2 = 1 ; \tag{B-5}$$

also,

$$C_T = C_1 + C_2 . \tag{B-6}$$

We may then write

$$C_T = \rho \left[(Y_1/M_1) + (Y_2/M_2) \right],$$

hence Equation (B-3) may be written in terms of weight fractions as

$$\bar{V}_1 - \bar{V}_2 = - D_{12} \frac{(M_2 Y_1 + M_1 Y_2)^2}{M_1 M_2 Y_1 Y_2} \nabla \left[\frac{M_2 Y_1}{M_2 Y_1 + M_1 Y_2} \right] . \tag{B-3a}$$

From Equations (B-2) and (B-5) we obtain

$$\bar{V}_1 - \bar{V}_2 = \frac{1}{Y_2} \bar{V}_1 , \tag{B-7}$$

and using Equation (B-7) in Equation (B-3a), we find that

$$\bar{V}_1 = - D_{12} \frac{(M_2 Y_1 + M_1 Y_2)^2}{M_1 M_2 Y_1} \nabla \left[\frac{M_2 Y_1}{M_2 Y_1 + M_1 Y_2} \right] . \tag{B-8}$$

After expanding the gradient term, Equation (B-8) may be written as

$$\bar{V}_1 = - \frac{D_{12}}{Y_1} (Y_2 \nabla Y_1 - Y_1 \nabla Y_2) . \tag{B-8a}$$

But

$$Y_1 + Y_2 = 1 ,$$

hence

$$\nabla Y_1 = - \nabla Y_2 .$$

Therefore, Equation (B-8a) reduces to

$$\bar{V}_1 = - \frac{D_{12}}{Y_1} \nabla Y_1, \qquad \text{(B-9)}$$

which is the desired result.

We now use Equations (B-4) and (B-9) in the conservation equation, Equation (B-1), to obtain

$$\partial(\rho Y_1)/\partial t = - \nabla \cdot [\rho Y_1 \bar{v} - \rho D_{12} \nabla Y_1] . \qquad \text{(B-10)}$$

For steady state conditions, the left-hand side of this equation is equal to zero, and it then follows that

$$\rho Y_1 \bar{v} - \rho D_{12} \nabla Y_1 = F(q) \qquad \text{(B-11)}$$

where $F(q)$ is some vector function of the coordinates, q, whose divergence is equal to zero. For a problem with spherical symmetry, this requirement is met only by the function

$$F(r) = \Gamma'/r^2 = \Gamma/4\pi r^2 , \qquad \text{(B-12)}$$

where Γ is a constant.

For the burning droplet problem,

$$\bar{v} = \dot{m}_F/4\pi r^2 \rho . \qquad \text{(B-13)}$$

After multiplying through by $4\pi r^2$, Equation (B-11) may now be written

$$Y_1 \dot{m}_F - 4\pi r^2 \rho D_{12} (dY_1/dr) = \Gamma. \qquad \text{(B-14)}$$

As it is apparent that the sum of mass transfer of species 1 resulting from the outward convection current, $Y_1 \dot{m}_F$, plus that due to diffusion, $- 4\pi r^2 \rho D_{12} (dY_1/dr)$, must equal the total rate of transfer of species 1, the constant Γ is simply equal to $\dot{m}_1$. This final integrated diffusion equation is identical to Equation (3), page 13.

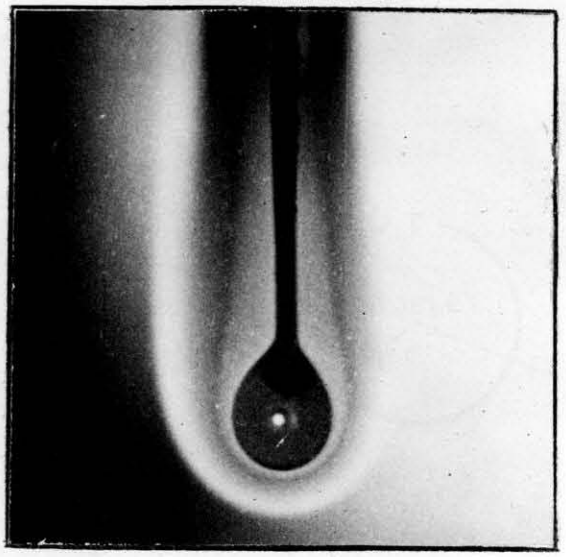

FIGURE 1 PHOTOGRAPH OF BENZENE DROPLET (~ 0.1 CM. DIAMETER) BURNING IN AIR.

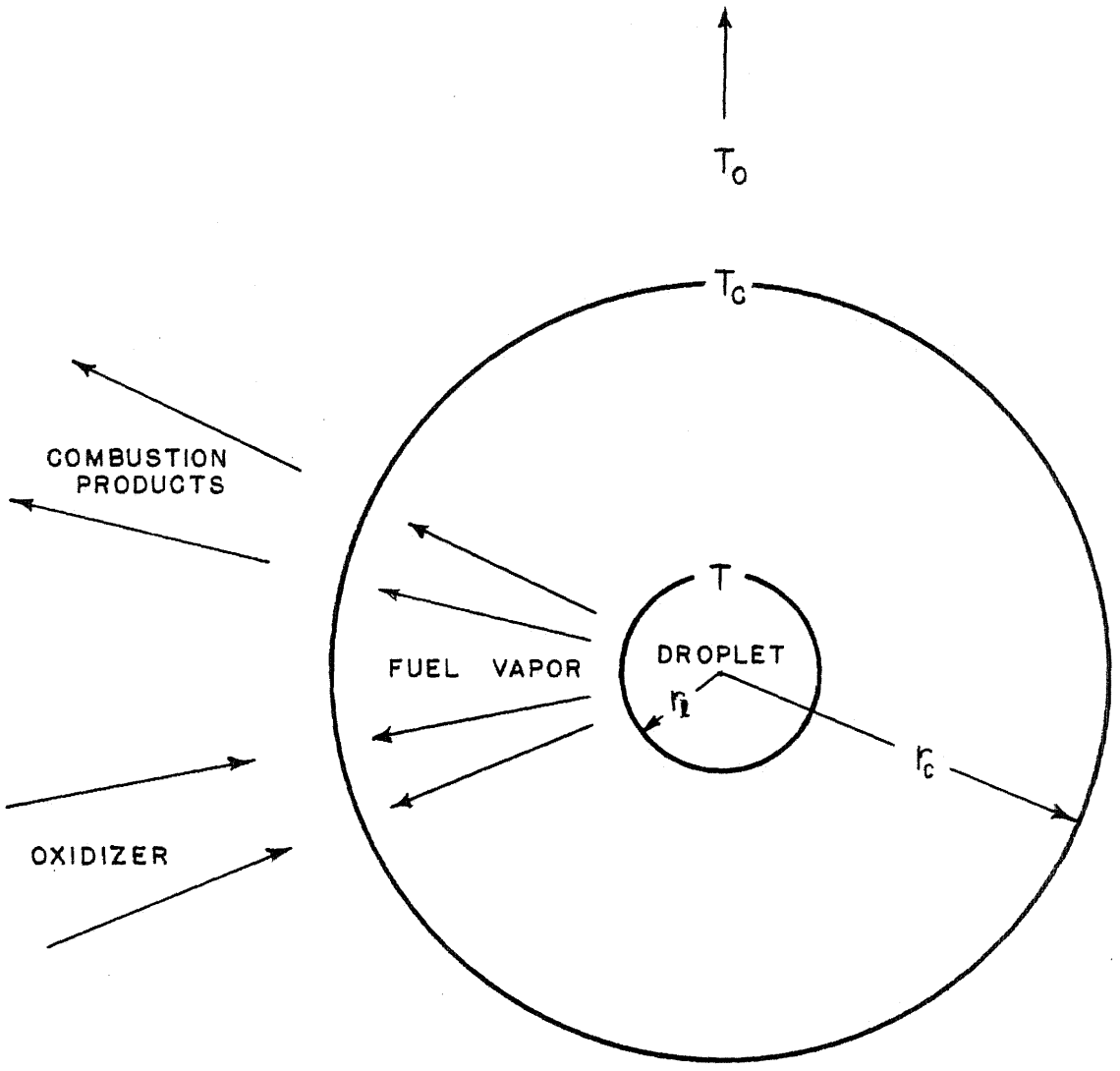

FIGURE 2 SCHEMATIC DIAGRAM OF MODEL FOR DIFFUSION THEORY OF DROPLET BURNING.

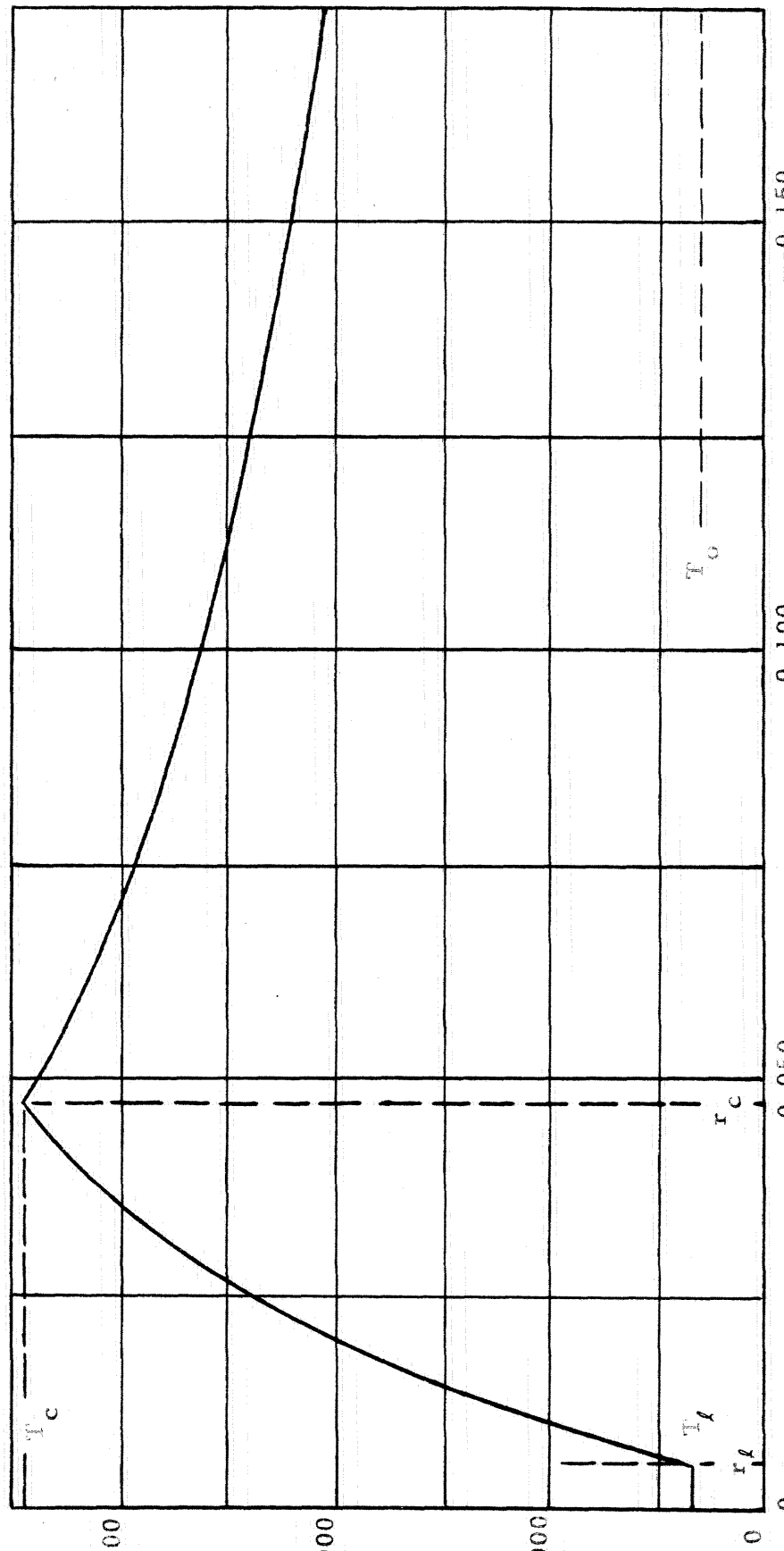

FIGURE 3a TEMPERATURE (T) AS A FUNCTION OF DISTANCE FROM CENTER OF DROP (r) FOR 0.010 CM. DIAMETER BENZENE DROPLET BURNING IN AIR AT ATMOSPHERIC PRESSURE ACCORDING TO DIFFUSION THEORY.

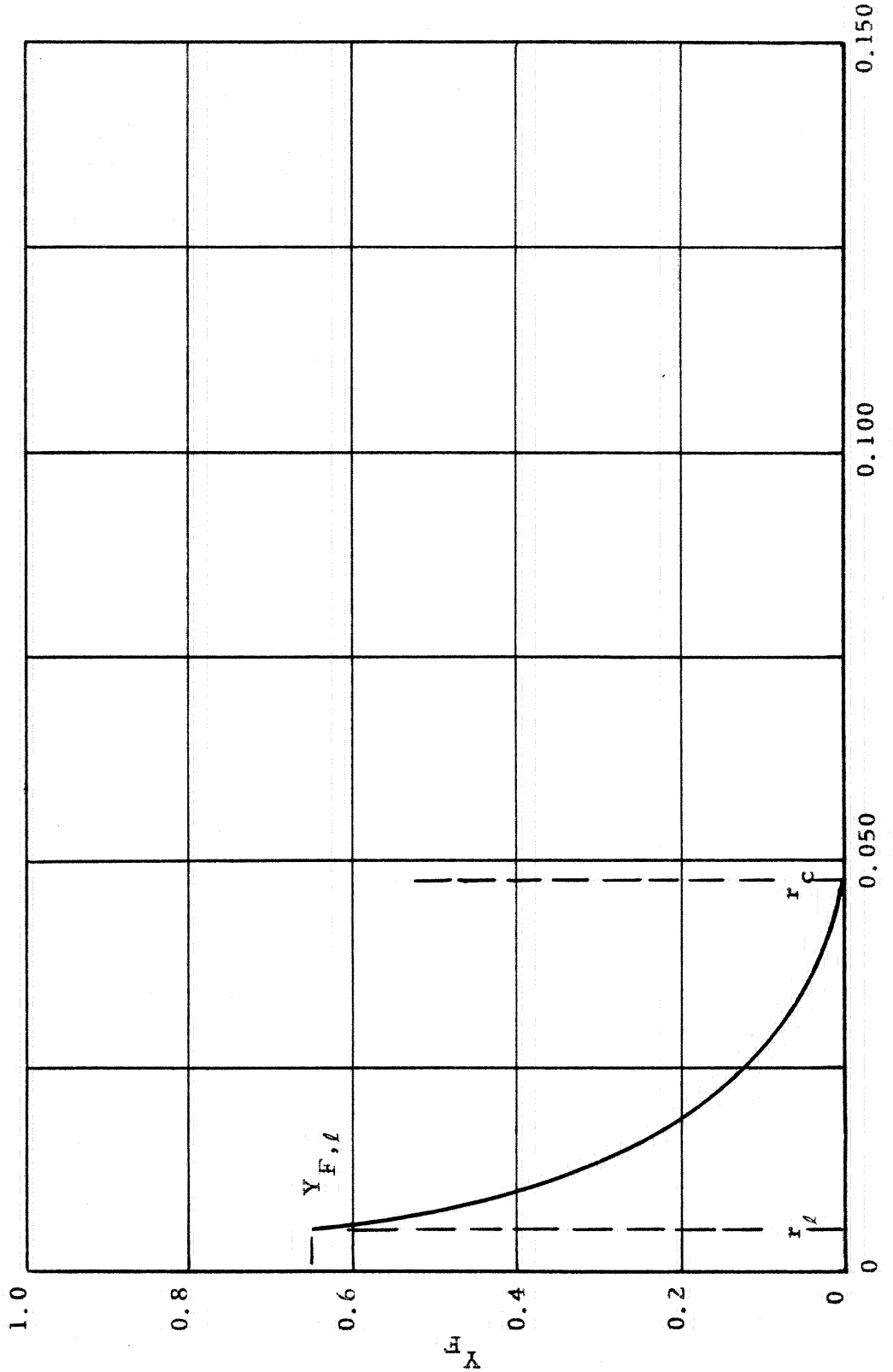

FIGURE 3b WEIGHT FRACTION OF FUEL VAPOR (Y_F) AS A FUNCTION OF DISTANCE FROM CENTER OF DROP FOR 0.010 CM. DIAMETER BENZENE DROPLET BURNING IN AIR AT ATMOSPHERIC PRESSURE ACCORDING TO DIFFUSION THEORY.

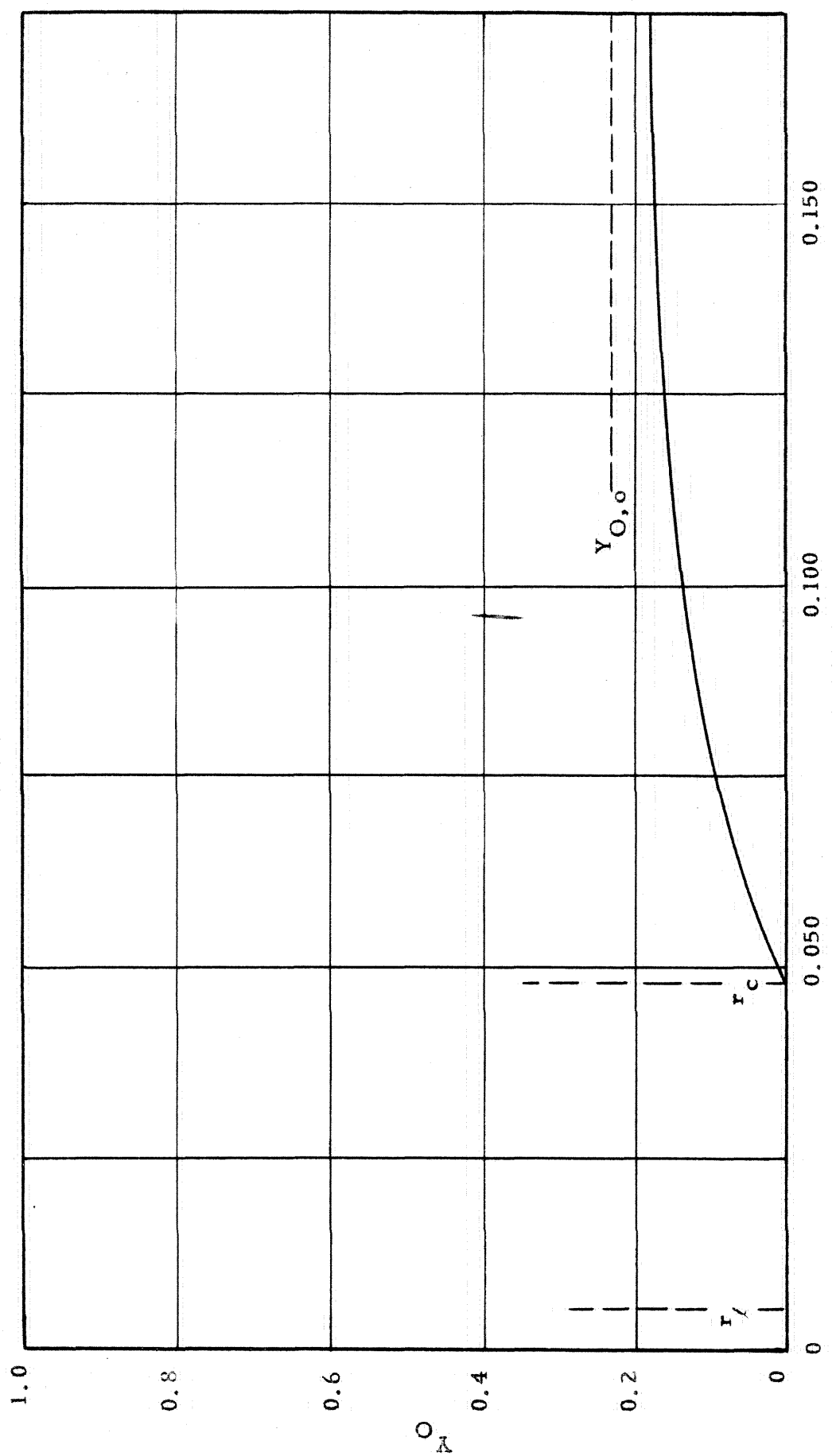

FIGURE 3c WEIGHT FRACTION OF OXYGEN (Y_O) AS A FUNCTION OF DISTANCE FROM CENTER OF DROP (r) FOR 0.010 CM. DIAMETER BENZENE DROPLET BURNING IN AIR AT ATMOSPHERIC PRESSURE ACCORDING TO DIFFUSION THEORY.

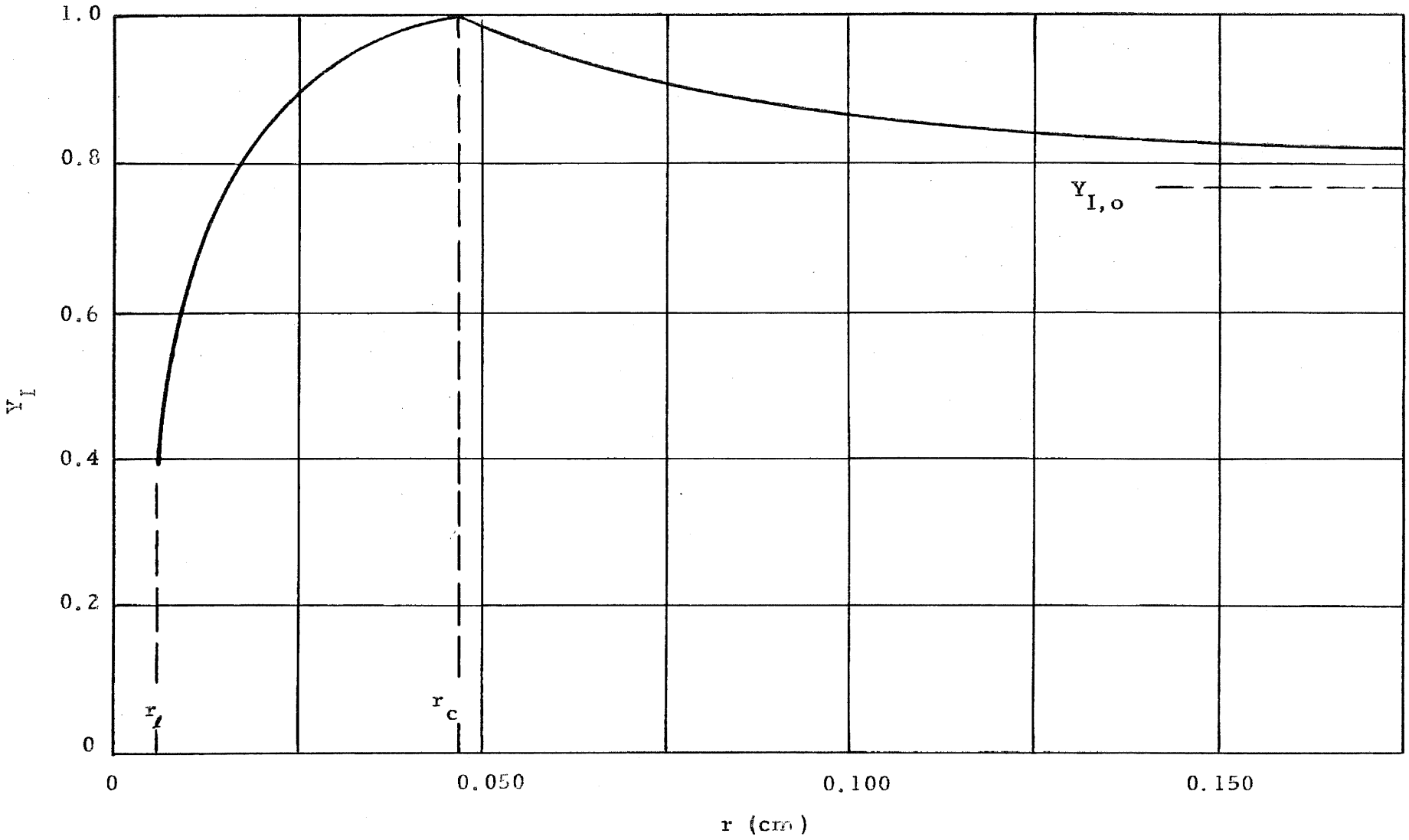

FIGURE 3d WEIGHT FRACTION OF INERT GAS (Y_I) AS A FUNCTION OF DISTANCE FROM CENTER OF DROP (r) FOR 0.010 CM. DIAMETER BENZENE DROPLET BURNING IN AIR AT ATMOSPHERIC PRESSURE ACCORDING TO DIFFUSION THEORY.

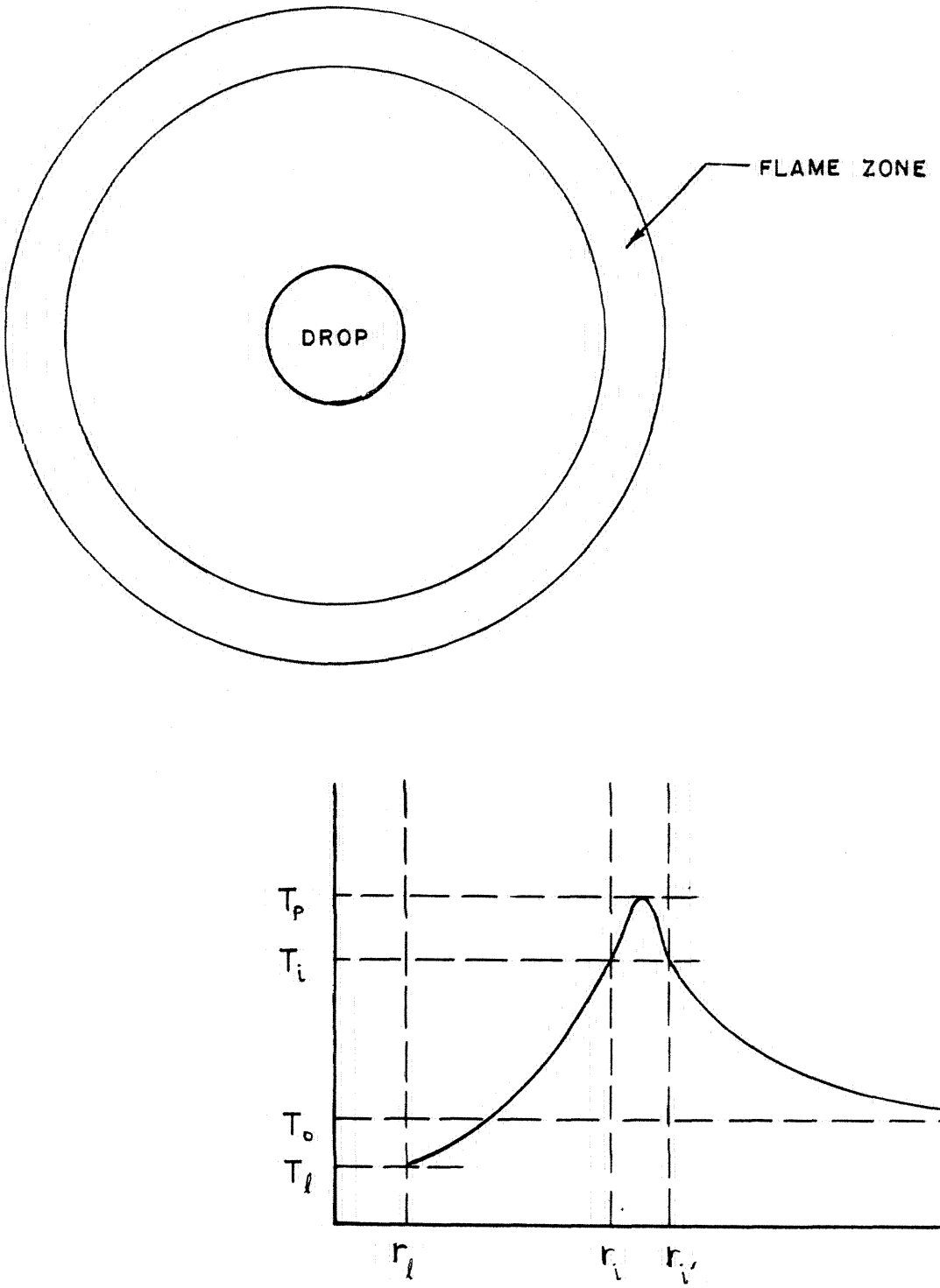

FIGURE 4 SCHEMATIC DIAGRAM OF MODEL AND TEMPERATURE PROFILE FOR THERMAL THEORY OF DROPLET COMBUSTION.

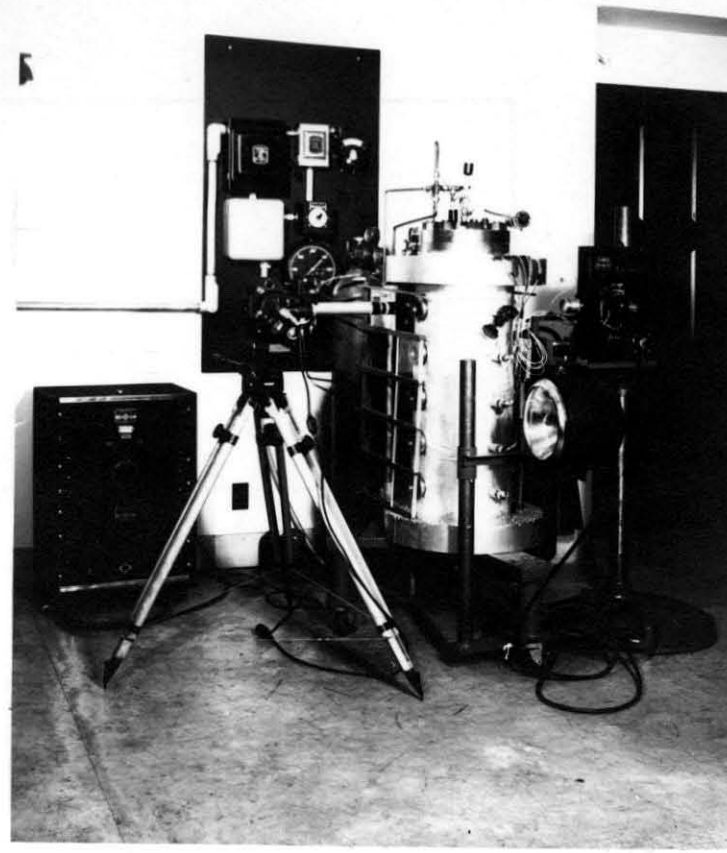

FIG. 5 COMBUSTION APPARATUS. "EYEMO" CAMERA IN LEFT CENTER. INJECTION AND IGNITION EQUIPMENT VISIBLE ON HEAD OF COMBUSTION TANK.

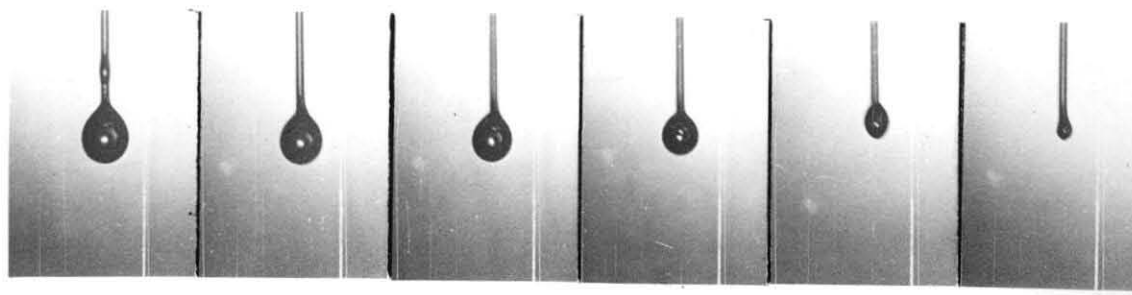

FIG. 6 DROPLET OF ETHYL ALCOHOL BURNING IN MIXTURE OF FIFTY PERCENT OXYGEN AND FIFTY PERCENT NITROGEN BY WEIGHT.

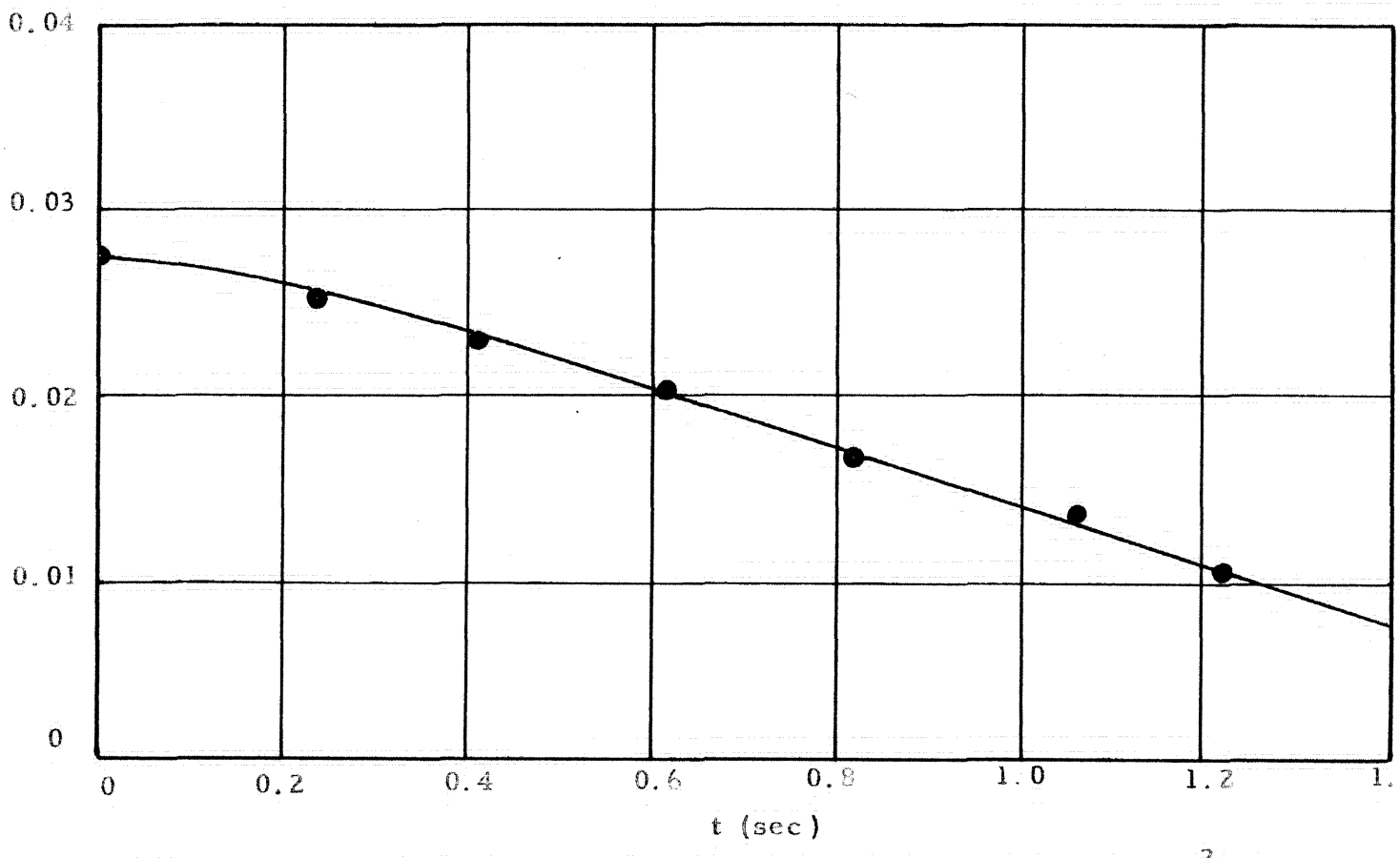

FIGURE 7 EXPERIMENTAL PLOT OF SQUARE OF DIAMETER (D^2) VS. TIME (t) FOR AN ETHYL ALCOHOL DROPLET BURNING IN OXYGEN - NITROGEN MIXTURE ($Y_{O,\infty} = 0.5$).

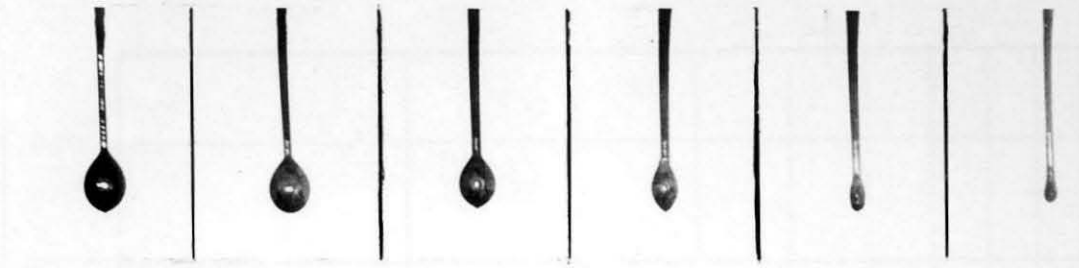

$Y_{O,o}$ = 0.23 (AIR)

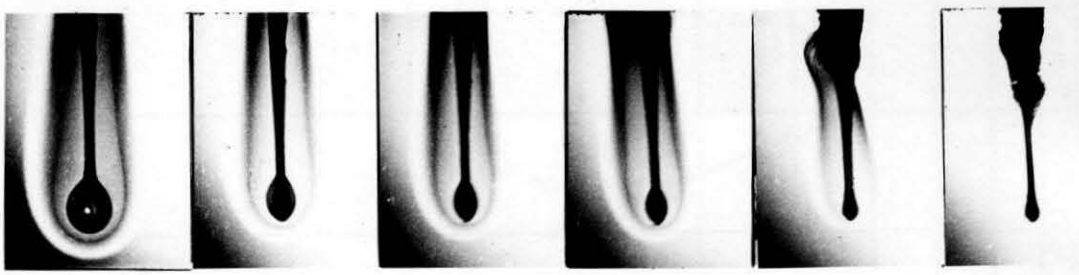

$Y_{O,o}$ = 0.30

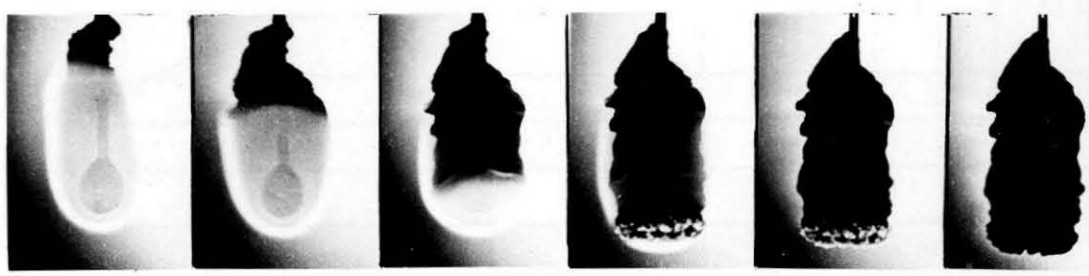

$Y_{O,o}$ = 0.50

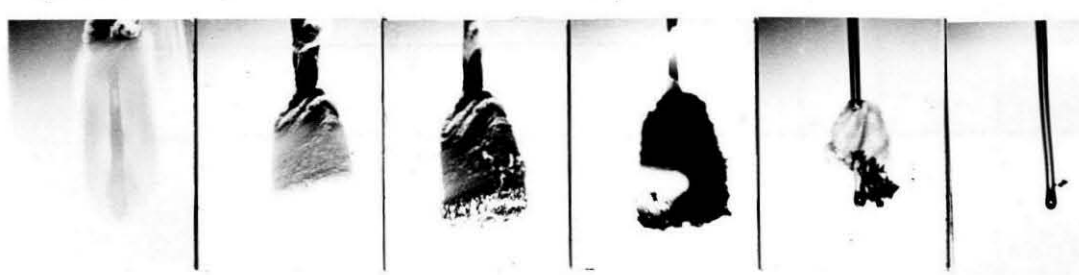

$Y_{O,o}$ = 0.70

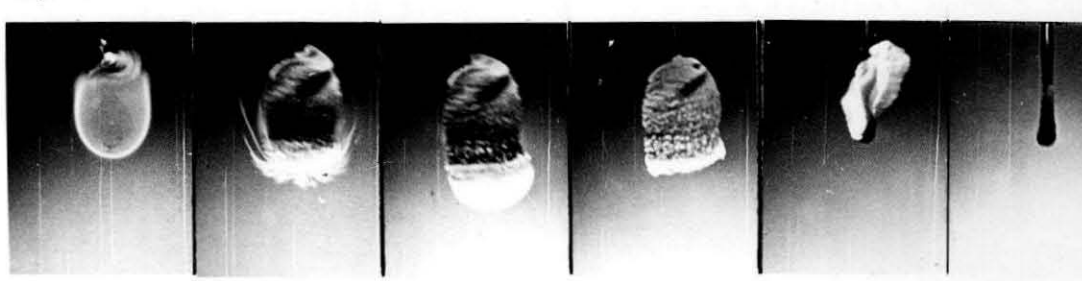

$Y_{O,o}$ = 0.90

FIG. 8 BENZENE DROPLETS BURNING IN VARIOUS OXYGEN - NITROGEN MIXTURES SHOWING RESIDUE FORMATION.

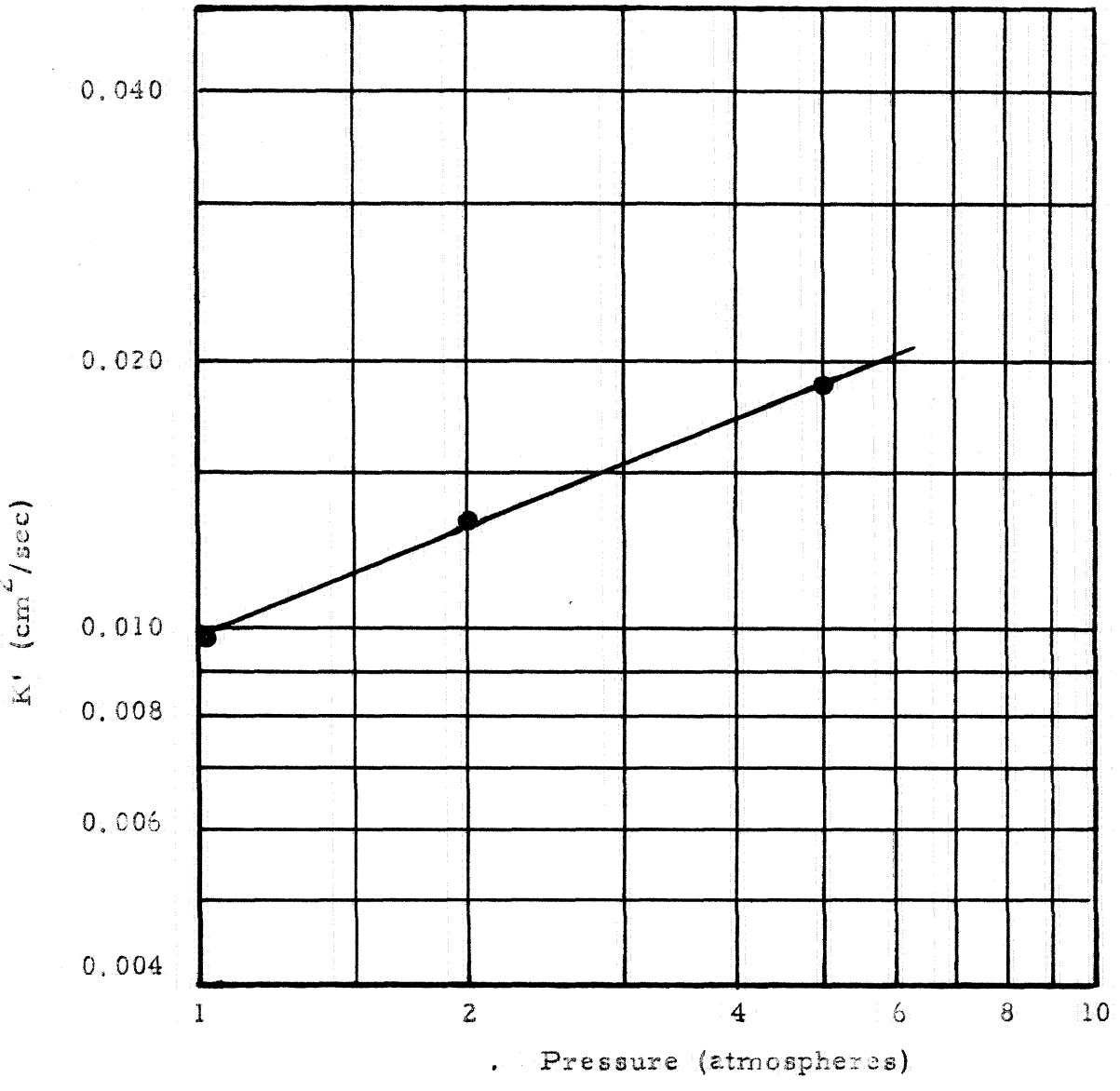

FIGURE 9 VARIATION OF EVAPORATION CONSTANT (K') WITH PRESSURE FOR BENZENE BURNING IN AIR.

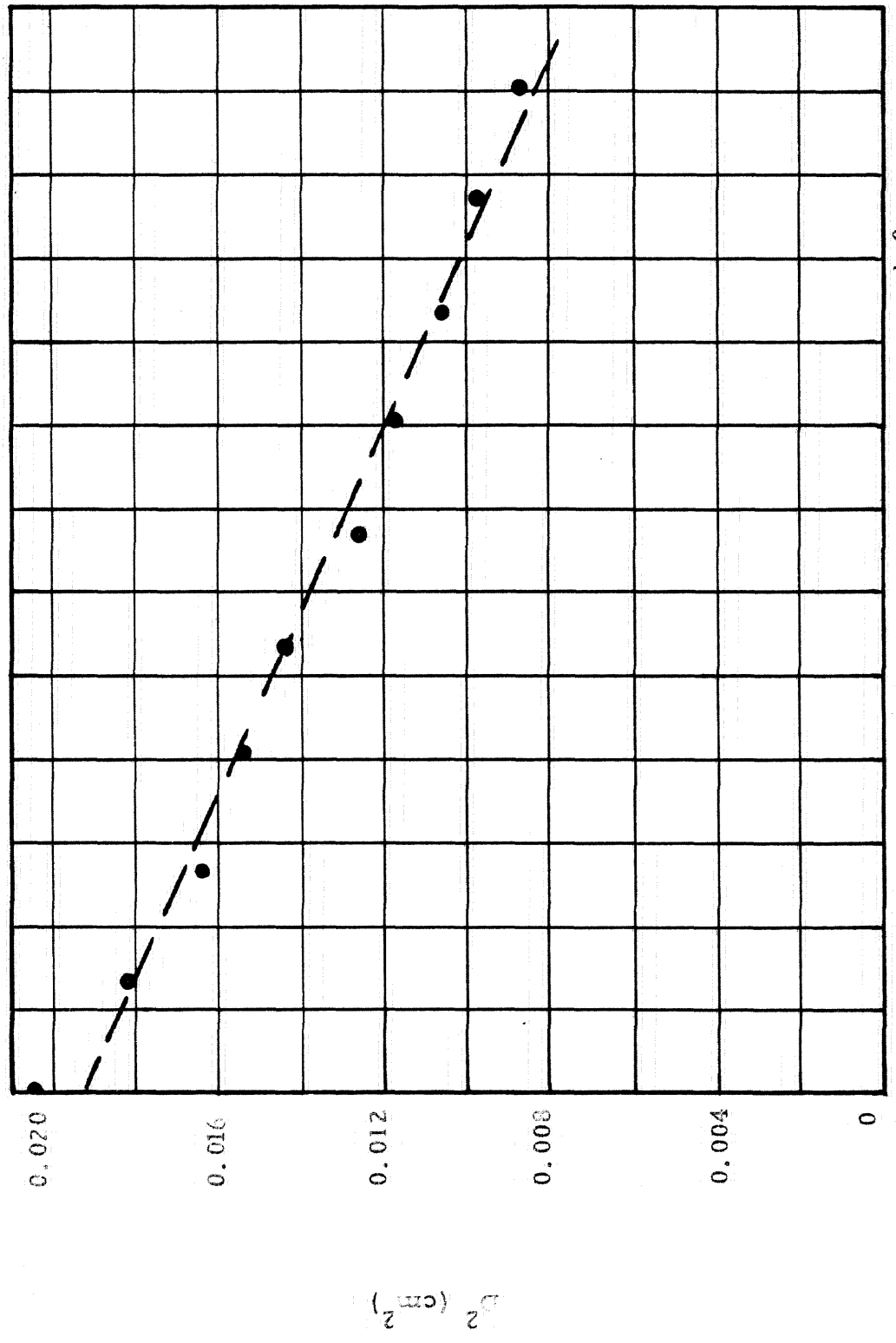

FIGURE 10 EXPERIMENTAL PLOT OF SQUARE OF DIAMETER (D^2) VS. TIME (t) FOR AN ETHYL ALCOHOL DROP BURNING IN AN AIR STREAM OF 11.6 CM/SEC VELOCITY.

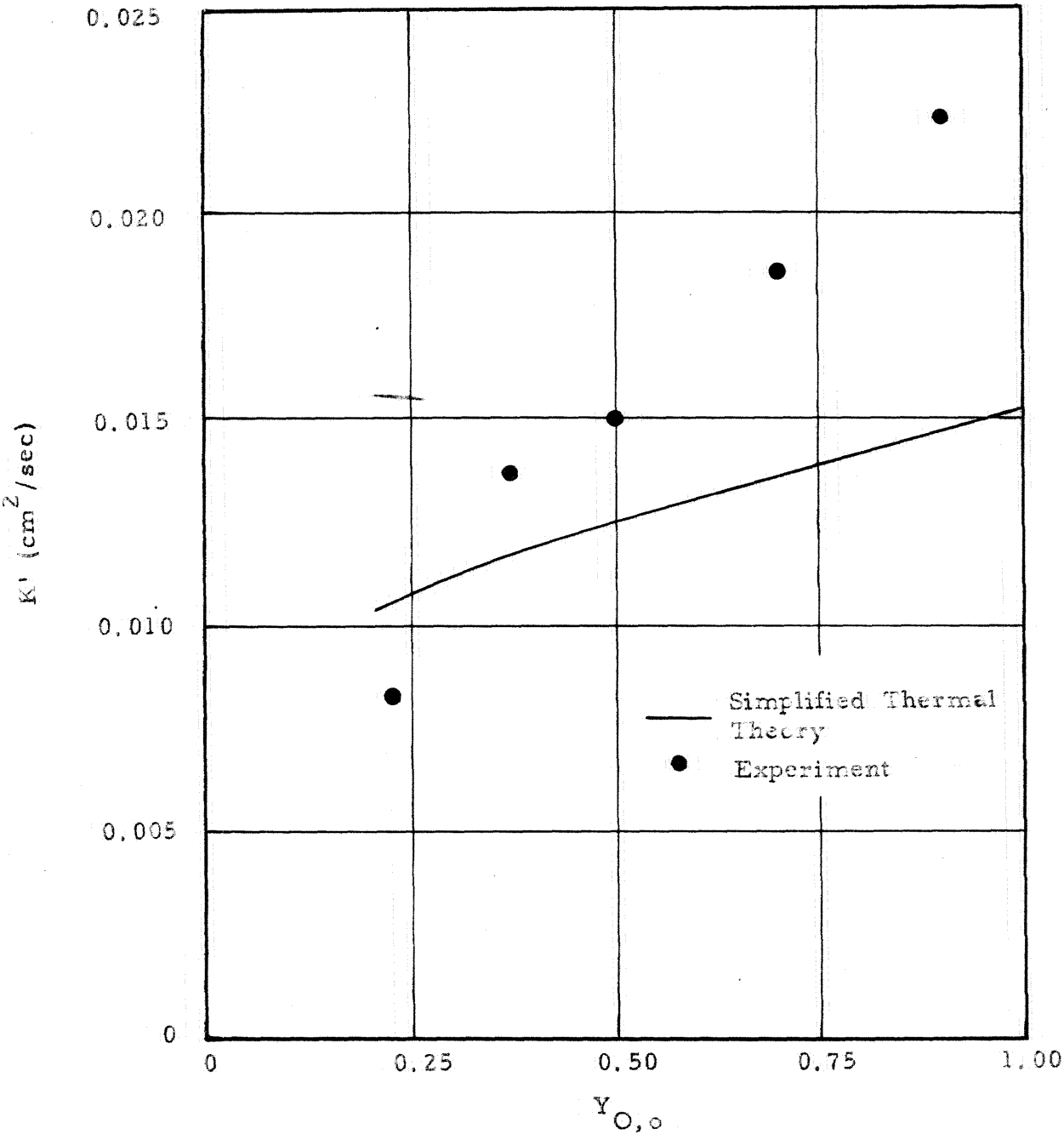

FIGURE 11 COMPARISON OF EXPERIMENTAL AND THEORETICAL VALUES FOR THE EVAPORATION CONSTANT (K') FOR N-HEPTANE BURNING IN VARIOUS OXYGEN-NITROGEN MIXTURES.

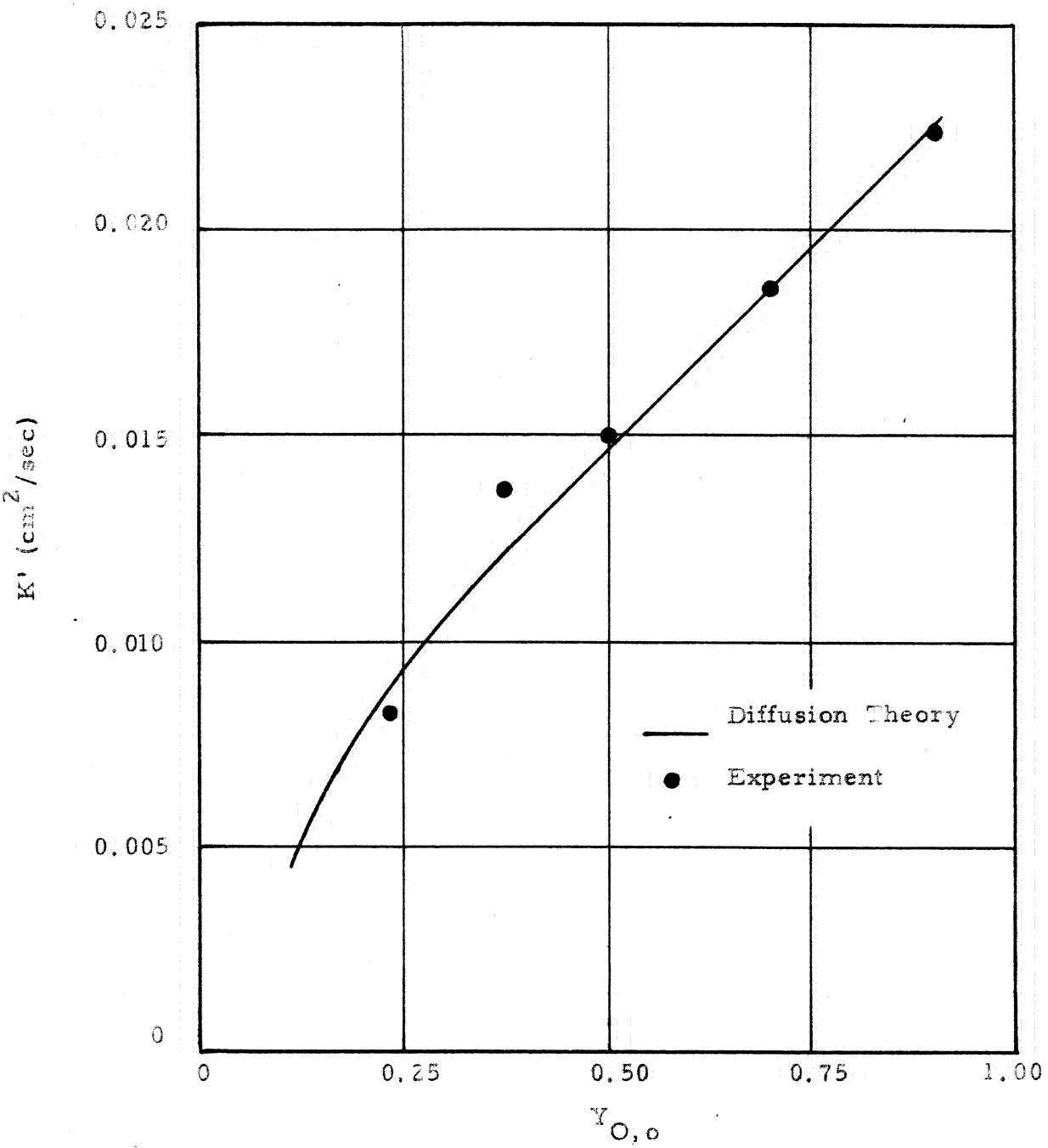

FIGURE 12 COMPARISON OF EXPERIMENTAL AND THEORETICAL VALUES FOR THE EVAPORATION CONSTANT (K') FOR N-HEPTANE BURNING IN VARIOUS OXYGEN-NITROGEN MIXTURES.

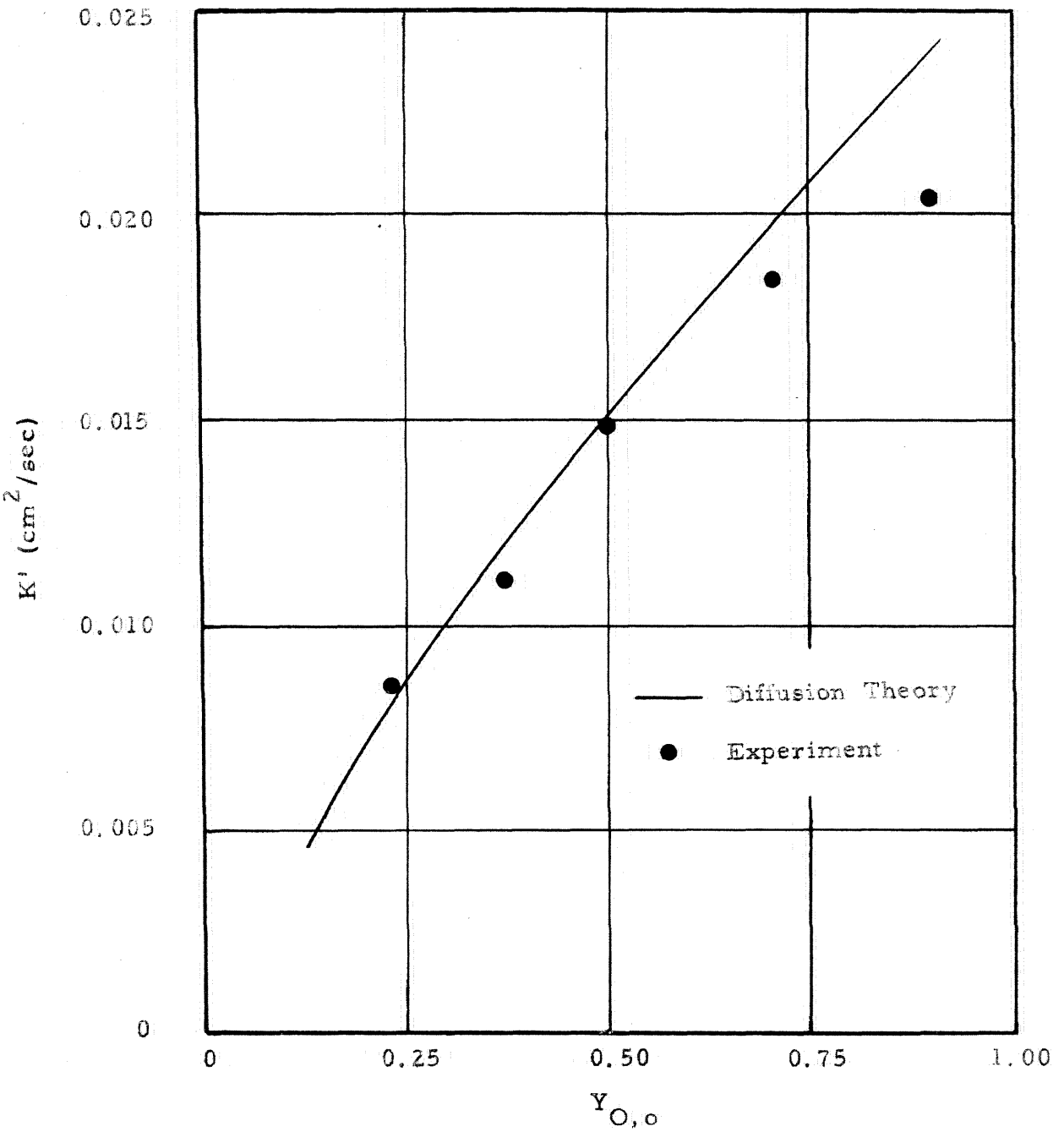

FIGURE 13 COMPARISON OF EXPERIMENTAL AND THEORETICAL VALUES FOR THE EVAPORATION CONSTANT (K') FOR ETHYL ALCOHOL BURNING IN VARIOUS OXYGEN-NITROGEN MIXTURES.

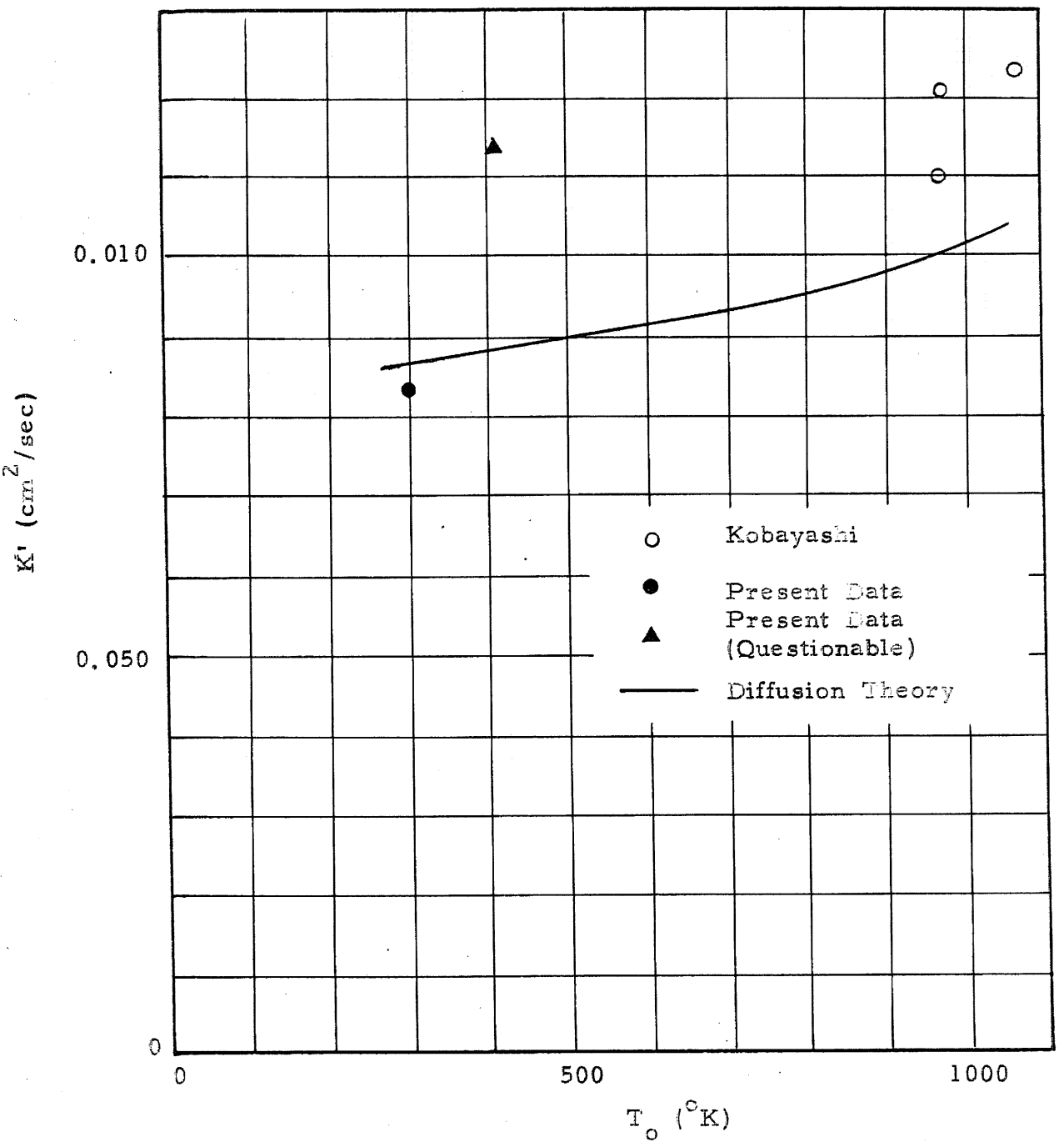

FIGURE 14 COMPARISON OF EXPERIMENTAL AND THEORETICAL VALUES OF THE EVAPORATION CONSTANT (K') FOR N-HEPTANE BURNING IN AIR AT VARIOUS AMBIENT TEMPERATURES.